Mon. Not. R. Astron. Soc. **000**, 000–000 (0000) Printed 2 February 2008 (MN LATEX style file v2.2)

Chandra observations of five ultraluminous X-ray sources in nearby galaxies

T. P. Roberts[1,*], R. S. Warwick[1], M. J. Ward[1] & M. R. Goad[2]
[1] *X-ray and Observational Astronomy Group, Dept. of Physics & Astronomy, University of Leicester, University Road, Leicester, LE1 7RH*
[2] *Dept. of Physics & Astronomy, University of Southampton, Highfield, Southampton, Hants., SO17 1BJ*
[*] *E-mail: tro@star.le.ac.uk*

ABSTRACT
We report the results of a programme of dual-epoch *Chandra* ACIS-S observations of five ultraluminous X-ray sources (ULXs) in nearby spiral galaxies. All five ULXs are detected as unresolved, point-like X-ray sources by *Chandra*, though two have faded below the 10^{39} erg s^{-1} luminosity threshold used to first designate these sources as ULXs. Using this same criterion, we detect three further ULXs within the imaged regions of the galaxies. The ULXs appear to be related to the star forming regions of the galaxies, indicating that even in "normal" spiral galaxies the ULX population is predominantly associated with young stellar populations. A detailed study of the *Chandra* ACIS-S spectra of six of the ULXs shows that five are better described by a powerlaw continuum than a multi-colour disc blackbody model, though there is evidence for additional very soft components to two of the powerlaw continua. The measured photon indices in four out of five cases are consistent with the low/hard state in black hole binaries, contrary to the suggestion that powerlaw-dominated spectra of ULXs originate in the very high state. A simple interpretation of this is that we are observing accretion onto intermediate-mass black holes, though we might also be observing a spectral state unique to very high mass accretion rates in stellar-mass black hole systems. Short-term flux variability is only detected in one of two epochs for two of the ULXs, with the lack of this characteristic arguing that the X-ray emission of this sample of ULXs is not dominated by relativistically-beamed jets. The observational characteristics of this small sample suggest that ULXs are a distinctly heterogeneous source class.

Key words: X-rays: galaxies - X-rays: binaries - Black hole physics

1 INTRODUCTION

Ultraluminous X-ray Sources (ULXs) can be broadly defined as the most luminous point-like extra-nuclear X-ray sources located within nearby galaxies, displaying X-ray luminosities in excess of 10^{39} erg s^{-1}. These sources were first observed in *Einstein* observations of nearby galaxies (e.g. Fabbiano & Trinchieri 1987), and more than one hundred were subsequently catalogued in *ROSAT* high-resolution imager observations (Roberts & Warwick 2000; Colbert & Ptak 2002). Whilst a fraction of this observed ULX population is associated with recent supernovae (e.g. SN 1986J, Bregman & Pildis 1992; SN 1979C, Immler, Pietsch & Aschenbach 1998), *ASCA* studies have shown that many ULXs appear to display the characteristics of accreting black holes (e.g. Makishima et al. 2000; Mizuno, Kubota & Makishima 2001). Crucially, high spatial resolution *Chandra* observations (e.g. Kaaret et al. 2001; Strickland et al. 2001), have failed to resolve most ULX targets. When combined with the observed significant flux variability, this suggests the presence of a single, luminous source of X-rays rather than a grouping of less luminous sources.

However, debate over the nature of the bulk of the ULX population is ongoing, since if these are accretion-powered sources their X-ray luminosities match, and in many cases greatly exceed, the Eddington limit for a typical stellar-mass (~ 10 M$_{\odot}$) black hole. Suggestions for their physical composition currently focus upon four possibilities. The first is that many ULXs are accreting examples of a new class of $10^2 - 10^5$ M$_{\odot}$ intermediate-mass black holes (IMBH; e.g. Colbert & Mushotzky 1999). The formation of such objects remains a matter of some debate; some intermediate-mass black holes may be the remnants of primordial Population III stars (e.g. Madau & Rees 2001), whilst others may be formed in dense globular clusters prior to being deposited in a galaxy disc (Miller & Hamilton 2002). An alternative scenario is that IMBH are formed by the runaway merger of stellar objects at the centre of young, dense stellar clusters (Ebisuzaki et al. 2001; Portegies Zwart & McMillan 2002). The existence of IMBH may be supported by the recent inferrence of 3×10^3 and 2×10^4 M$_{\odot}$ massive dark objects in the cores of the globular clusters M15 and G1 respectively (van der Marel et al. 2002; Gerssen et al. 2002; Gebhardt et al. 2002), though the presence of such an object in M15 is far from proven (Baumgardt et al. 2002). Further evidence has recently emerged with the discovery of the X-ray spectral signature

of "cool" accretion discs, consistent with the presence of IMBH, in several ULXs (e.g. Miller et al. 2003, Roberts & Colbert 2003).

The remaining models focus upon interpreting ULXs as extreme examples of "ordinary" stellar-mass (i.e. ~ 10 M$_\odot$) black hole X-ray binaries. The second physical model is that many ULXs are ordinary X-ray binaries in an unusually high accretion mode, in which their accretion disc becomes radiation pressure-dominated, producing photon bubble instabilities that allow the disc to radiate at a truly super-Eddington X-ray flux (Begelman 2002). Thirdly, many ULXs may only appear to exceed the Eddington limit, but could in fact be X-ray binaries emitting anisotropically (King et al. 2001), with only a mild beaming factor $b \sim 0.1$ (where $b = \Omega/4\pi$, and Ω is the solid angle of the X-ray emission) required in most cases to reduce the energy requirements below the Eddington limit for a conventional stellar-mass black hole. The fourth model is a variation on the third scenario, suggested by Reynolds et al. (1997) and more recently Körding, Falcke & Markoff (2001) and Georganopoulos, Aharonian & Kirk (2002), in which ULXs are microquasars in nearby galaxies that we are observing directly down the beam of their relativistic jet ("microblazars", c.f. Mirabel & Rodriguez 1999). Observational support for this last scenario comes from the detection of radio emission, potentially the signature of a relativistically-beamed jet, emanating from an ULX in NGC 5408 (Kaaret et al. 2003).

Current observations do not completely rule out any of the above scenarios. However, they do suggest that there may be at least two separate underlying populations of ULXs, since a large number are seen coincident with active star formation regions (e.g. Zezas & Fabbiano 2002; Roberts et al. 2002) and hence are presumably associated with nascent stellar populations, whereas some ULXs are found in elliptical galaxies (e.g. Irwin, Athey & Bregman 2003) and so must be associated with an older stellar population. King (2002) suggests that the population associated with star formation are high-mass X-ray binaries (HMXBs) undergoing an episode of thermal-timescale mass transfer (see also King et al. 2001), whilst the older population may be long-lasting transient outbursts in low-mass X-ray binaries. Local examples of each suggested class are SS 433 and GRS 1915+105 respectively. This heterogeneity is supported by the first reported optical stellar counterparts to ULXs. Roberts et al. (2001) report the detection of a blue continuum source coincident with NGC 5204 X-1, which *HST* resolved into three separate sources with colours that are consistent with young, compact stellar clusters in NGC 5204 (Goad et al. 2002). *HST* observations also show an ULX in M81 (NGC 3031 X-11) to have a possible O-star counterpart (Liu et al. 2002). In contrast, ULXs have been found with potential globular cluster counterparts in both NGC 4565 (Wu et al. 2002) and NGC 1399 (Angelini, Loewenstein & Mushotzky 2001), suggesting that these ULXs are associated with the older stellar population, or perhaps massive central black holes, of these globular clusters.

In this paper, we present the results of dual-epoch *Chandra* observations of five different ULXs located in nearby ($d < 10$ Mpc) galaxies, awarded *Chandra* time in AO-2 & AO-3. These ULXs are listed in Table 1. They were selected from the catalogues of *ROSAT* HRI point-like X-ray source detections in nearby galaxies presented by Roberts & Warwick (2000; hereafter RW2000) and Lira, Lawrence & Johnson (2000) on the basis of their high X-ray luminosities ($\mathrm{L_X} > 10^{39}\ \mathrm{erg\,s^{-1}}$ in the *ROSAT* HRI) and the lack of previous *Chandra* observations. A discussion of the observational history of these ULXs is presented in Appendix A. Further discussion of the environment of each of these ULXs, as determined from William Herschel Telescope/INTEGRAL IFU observations, will be detailed in a future paper (Roberts et al., in prep.).

Table 2. The host galaxies.

Galaxy	Hubble type[a]	d^b (Mpc)	i^b (°)	$N_H{}^c$ ($\times 10^{20}$ cm^{-2})
IC 342	SAB(rs)cd	3.9	20	30.3
NGC 3628	SAb pec sp	7.7	87	2.0
NGC 4136	SAB(r)c	9.7	0[d]	1.6
NGC 4559	SAB(rs)cd	9.7	69	1.5
NGC 5204	SA(s)m	4.8	53	1.5

Notes:
[a] Data from the NASA/IPAC extragalactic database (NED).
[b] Distance (d) and inclination (i) data from Tully (1988).
[c] Foreground absorption, interpolated at the position of each galaxy from the HI maps of Stark et al. (1992).
[d] There is no recorded inclination, so a face-on aspect is adopted after inspection of Digitised Sky Survey images.

The layout of this paper is as follows. In the next section we briefly outline the details of the *Chandra* observations and the data reduction. This is followed by a discussion of the detection of these (and three other) ULXs, and their locations within their host galaxies. In section 4 we detail the spatial, temporal and spectral properties of each source, before discussing the implications of these results for possible physical models of ULXs in section 5. Our findings and conclusions are summarised in section 6.

2 CHANDRA OBSERVATIONS AND DATA REDUCTION

The details of the ten *Chandra* observations of ULXs that form the basis of this paper are listed in Table 1. The observations were pointed at the *ROSAT* HRI positions of the ULXs, after a correction to the astrometry calculated from X-ray/optical matches in the HRI field-of-view. All coordinates listed in the Table, and throughout this paper, are epoch J2000. We tabulate some basic parameters for the host galaxies in Table 2. The observations were performed between 2001 January 9 and 2002 August 26, and range in exposure time from 9.7 to 22.5 ks. Each target was observed on two occasions, separated by 3 – 5 months. In order to mitigate the anticipated effects of detector pile-up in the ACIS-S S3 chip, several of the observations were performed in a sub-array mode; these are listed in Table 1. The choice of sub-array was governed by the anticipated count rates, modelled from the previous *ROSAT* HRI observations of these objects (RW2000; Lira, Lawrence & Johnson 2000), with the aim of limiting the pile-up fraction to 10% or less in each observation. On this basis, sub-arrays were deemed necessary for three of the five targets in the programme.

Data reduction was performed using the CIAO software suite, versions 2.1 and 2.2. The reduction started in each case with the level two event file, from which events with energies outside the 0.3 – 10 keV range were rejected. All datasets were searched for periods of high background flaring, but none were observed, allowing the full science exposure to be utilised in each case. Further steps in the analysis of the data are outlined in the following sections.

3 ULX DETECTIONS AND LOCATIONS

A 0.3 – 10 keV image of the central $8.1' \times 8.1'$ region of each field was constructed from the corresponding cleaned event file. This im-

Table 1. Details of the ten *Chandra* observations.

Target	Observation aimpoint		*Chandra* sequence number	Observation date	ACIS-S3 subarray	Exposure
	Right ascension	Declination		(yyyy-mm-dd)		(ks)
IC 342 X-1	$03^h45^m55.2^s$	$+68°04'55''$	600253	2002-04-29	$\frac{1}{8}$	9.9
			600254	2002-08-26		9.9
NGC 3628 X-2	$11^h20^m37.5^s$	$+13°34'28''$	600255	2002-04-06	*full*	22.3
			600256	2002-07-04		22.5
NGC 4136 X-1	$12^h09^m22.6^s$	$+29°55'49''$	600257	2002-03-07	*full*	18.8
			600258	2002-06-08		19.7
NGC 4559 X-1	$12^h35^m52.0^s$	$+27°56'01''$	600160	2001-01-14	$\frac{1}{4}$	9.7
			600161	2001-06-04		11.1
NGC 5204 X-1	$13^h29^m39.2^s$	$+58°25'01''$	600162	2001-01-09	$\frac{1}{8}$	10.1
			600163	2001-05-02		9.5

age was searched for point sources using WAVDETECT, a wavelet-based source detection algorithm available in the CIAO package, and the X-ray source detections coincident with the optical extent of each galaxy (or that part of it within the ACIS-S3 field-of-view) were catalogued. The target ULXs were detected in every observation, and their *Chandra* nomenclature[1], including their refined position, and observed count rates are listed in Table 3. Count rates were converted to approximate fluxes based on a simple powerlaw continuum model with a standard photon index (Γ) of 2, subject to a foreground absorption column appropriate for each galaxy (see Table 2). In addition to the targets, three other sources with luminosities potentially in the ULX regime were found; one is a previously catalogued source (NGC 4559 X-4 in RW2000), but the other two are new ULX identifications. The details of these new ULXs are also given in Table 3.

One excellent capability of the *Chandra* observatory is that it provides an absolute astrometry solution to an accuracy of one arcsecond or better. This positional accuracy facilitates detailed follow-up of the *Chandra* X-ray source detections through the characterisation of their multi-wavelength counterparts. This avenue has already borne fruit in the study of ULXs, as discussed in the introduction. However, here we limit ourselves to a brief discussion of the environment of the *Chandra* ULX detections on the basis of Palomar Digitised Sky Survey (DSS) data.

The positions of the ULXs relative to their host galaxies are illustrated in Figures 1 & 2, where we overlay the *Chandra* X-ray emission contours onto DSS-2 (blue) images of the equivalent field-of-view. In each case the target ULX is at the centre of the field-of-view. The position of each ULX with respect to the nucleus of the parent galaxy is quantified in Table 3. The observed offset from the position of the galaxy nucleus, taken in each case from Falco et al. (1999), is simply the projected distance measured in arcseconds; we correct this to a deprojected radius, assuming that each source is in the plane of its host galaxy, using the host's inclination as given in Table 2 and a position angle taken from the RC3 catalogue (de Vaucouleurs et al. 1991). This deprojected radius is also shown as $f(R_{25})$, the fraction of the distance between the nucleus and the edge of the galaxy, defined by the semi-major axis of the 25 mag arcsec^{-2} isophotal ellipse, at which the ULX is found. Finally, we also give a qualitative description of the region of the galaxy in which the ULX is found.

If the ULXs in these galaxies are associated with young stellar populations, we might expect to find them co-located with the regions of the galaxy most prone to hosting star formation, such as the spiral arms, whereas if they are associated with the older stars then their distribution is more likely to be centrally peaked, or spread evenly throughout the disc. Table 2 shows that the majority of the ULXs (five out of eight) are located more than halfway out from the nucleus towards the edge of the galaxy. Four out of these five appear coincident with spiral arms; the fifth (CXOU J112037.3+133429) is located in an edge-on system where we cannot distinguish whether it is in an arm, or an inter-arm region.

The identification of four of the ULXs with spiral arms is relatively robust, as in both IC 342 and NGC 4136 the galaxies are face-on and so line-of-sight confusion through the galaxy is minimised. This is also true for CXOU J123551.7+275604 in NGC 4559, as this is located in a faint outer spiral arm clearly separated in projection from the main body of the galaxy. The co-location of the ULXs with spiral arms itself argues that they could be associated with a young stellar population. If they are ordinary X-ray binaries, with typical kicks imparted from the formation of the compact primary in a supernova explosion of $\sim 100\ \mathrm{km\ s^{-1}}$ (c.f. recent results for GRO 1655-40, Mirabel et al. 2002), then in 10^7 years this would move the position of the ULX relative to its birth place by a maximum of 1 kpc, consistent with an observed position in or near a spiral arm if born there. However, if the ULX are associated with an older population then in their $> 10^8$ year lifetime they could be displaced by 10 kpc or more, clearly leaving no requirement for an association with the spiral arms. The arguments in favour of these ULXs being related to young stellar populations are supported by follow-up observations of the immediate environments of three of these "outer" ULXs, with HII regions detected close to (within 200 pc of) CXOU J123551.7+275604 and coincident with CXOU J120922.6+295551 (Roberts et al., in prep.), and the detection of a possible supernova remnant encircling the position of CXOU J034555.7+680455 (Roberts et al. 2003). However, the kick argument above requires that either the ULXs are very young, or possess a small kick velocity and/or a velocity almost entirely projected along our line-of-sight for these to be true physical associations rather than line-of-sight coincidences with the star formation regions we might expect to observe within a galaxy's spiral arms.

Line-of-sight confusion is a much bigger issue for the three ULXs that are located closer to the centre of their respective host galaxies. Despite this, detailed follow-up of CXOU J132938.6+582506 reveals it to be associated with young stars (Goad et al. 2002). The remaining two sources are located close to the centre of NGC 4559. However, the nucleus of this galaxy

[1] We refer to the ULXs by their *Chandra* names throughout this paper. The cross-identification with previous names is shown where necessary.

Table 3. The ULX detections.

CXOU J	Previous designation	Count rate (ct ks^{-1}) Epoch 1	Epoch 2	Offset from galaxy nucleus observed ($''$)	deprojected (kpc)	$f(R_{25})$	Location
Targetted ULX							
034555.7+680455	IC 342 X-1	212 ± 5	226 ± 5	302	6.1	0.68	Spiral arm
112037.3+133429	NGC 3628 X-2	13 ± 1	13 ± 1	292	10.8	0.66	Outer disc
120922.6+295551	NGC 4136 X-1	3 ± 1	4 ± 1	65	3.0	0.54	Spiral arm
123551.7+275604	NGC 4559 X-1	153 ± 4	192 ± 4	123	15.2	0.96	Faint outer spiral arm
132938.6+582506	NGC 5204 X-1	411 ± 6	159 ± 4	17	0.7	0.21	Inner disc
Field ULX							
120922.2+295600	-	26 ± 1	18 ± 1	62	2.9	0.52	Spiral arm
123557.8+275807	-	11 ± 1	21 ± 1	31	2.3	0.15	Inner disc
123558.6+275742	NGC 4559 X-4	62 ± 3	119 ± 3	12	1.7	0.11	Inner disc/bulge

is known to host active star formation (Ho, Filippenko & Sargent 1997), implying that it is possible (though by no means certain) that these ULXs may also be related to the presence of young stars. It is entirely plausible, then, that all the ULXs in this small sample may be associated with young stellar populations. This is consistent with previous studies finding comparatively large populations of ULX in the most active star forming galaxies (e.g. Fabbiano, Zezas & Murray 2001; Lira et al. 2002; Zezas, Ward & Murray 2003), indicating a relationship between many ULX and active star formation, though interestingly in this case we co-locate them with the star forming regions of otherwise relatively normal galaxies.

To put this in context, it is worth noting that the host galaxies in our sample are all type Sb or later, indicating that they are disc-dominated, and so do not possess large bulges dominated by old stars. We can investigate the ULX – young stellar population link further by reference to the ULX survey of Colbert & Ptak (2002). They detect more than 30 candidate ULXs coincident with, or in the haloes of, elliptical galaxies, which must be dominated by an old stellar population. Averaging over the fourteen elliptical galaxies in which ULXs are located with respect to the blue luminosity of each galaxy, L_B, gives 0.8 ULX per 10^{10} L_B. This is very much an *upper* limit on the number of ULX from an old stellar population, as Colbert & Ptak search out to a radius of $2R_{25}$, potentially allowing a much greater contamination from background objects than simply focussing within the standard definition of the galaxy size, the 25 mag arcsec^{-2} isophotal ellipse. Also, since many of their candidate ULXs are possible halo objects, these may therefore constitute a physically separate population to that associated with the old stellar population. Nevertheless, by comparing their average ULX to L_B ratio with the blue luminosities of our target galaxies (and correcting for the coverage of each galaxy in the *Chandra* observations), we can establish a conservative upper limit on the number of our ULXs associated with the older stellar populations. This turns out to be an upper limit of two out of the eight ULXs we observe. We therefore confirm that our sample is very likely to be dominated by ULXs associated with a young stellar population.

4 X-RAY CHARACTERISTICS

In this section we investigate the detailed X-ray properties of the sources. Unless specifically stated, we perform the analyses on all five target plus all three field ULXs. Discussion of these characteristics in terms of physical models is deferred until later sections.

4.1 Spatial extent

A primary goal of this programme was to use the unique 0.5-arcsecond spatial resolution of *Chandra* to investigate whether these ULXs are resolved into complexes of many X-ray emitting sources, or whether they remain a single, point-like object at the highest available X-ray resolution. Hence, the target ULXs were placed at the on-axis aimpoint of the ACIS-S3 chip in each observation to provide the best possible spatial data.

To investigate the question of spatial extension, the two observations of each field were combined to enhance the signal-to-noise ratio of the images. The excellent spatial precision of the data (1 pixel $\equiv$ 0.492 arcsecond) was maintained by lining-up the peak in intensity of each target source. This method was verified by examining the peaks in fainter sources within the field, which also lined-up accurately. We then derived the radial profile of each ULX and fit its core with a Gaussian function, following the procedure described in section 4.2.1 of Roberts et al. (2002)[2]. The resulting fits gave FWHM of between 1.8 – 2.2 pixels for all on-axis sources, and ~ 2.4 pixels for the 2-arcmin off-axis ULXs in NGC 4559, all consistent with the nominal *Chandra* point-spread function at those positions. No evidence was found for a faint, extended component surrounding the position of any of the ULXs. This demonstrates that the ULXs are point-like at the 0.5-arcsecond spatial resolution of *Chandra*, corresponding to maximum physical sizes for the X-ray emitting regions of ~ 9 – 23 parsecs in the host galaxies. The spatial data is also, of course, consistent with all the objects being single, point-like X-ray sources.

4.2 Spectral properties

Spectra were extracted in an eight arcsecond diameter aperture centred on the position of each ULX using the PSEXTRACT script, which also retrieves the appropriate response matrices and ancillary response files for each observation. A source-free local background region of equivalent size was used in each case, though its impact was of little significance since it typically contained only $0.1 - 1\%$ of the counts accumulated from the source. The ancillary response files were corrected for the gradual in-orbit degradation in the quantum efficiency of the ACIS detectors using the CORRARF

[2] Some adjustments to the size and position of the background annuli were required to eliminate nearby X-ray sources in several fields. An example is the NGC 4136 field, in which the two ULXs are separated by only $\sim$ 22 pixels.

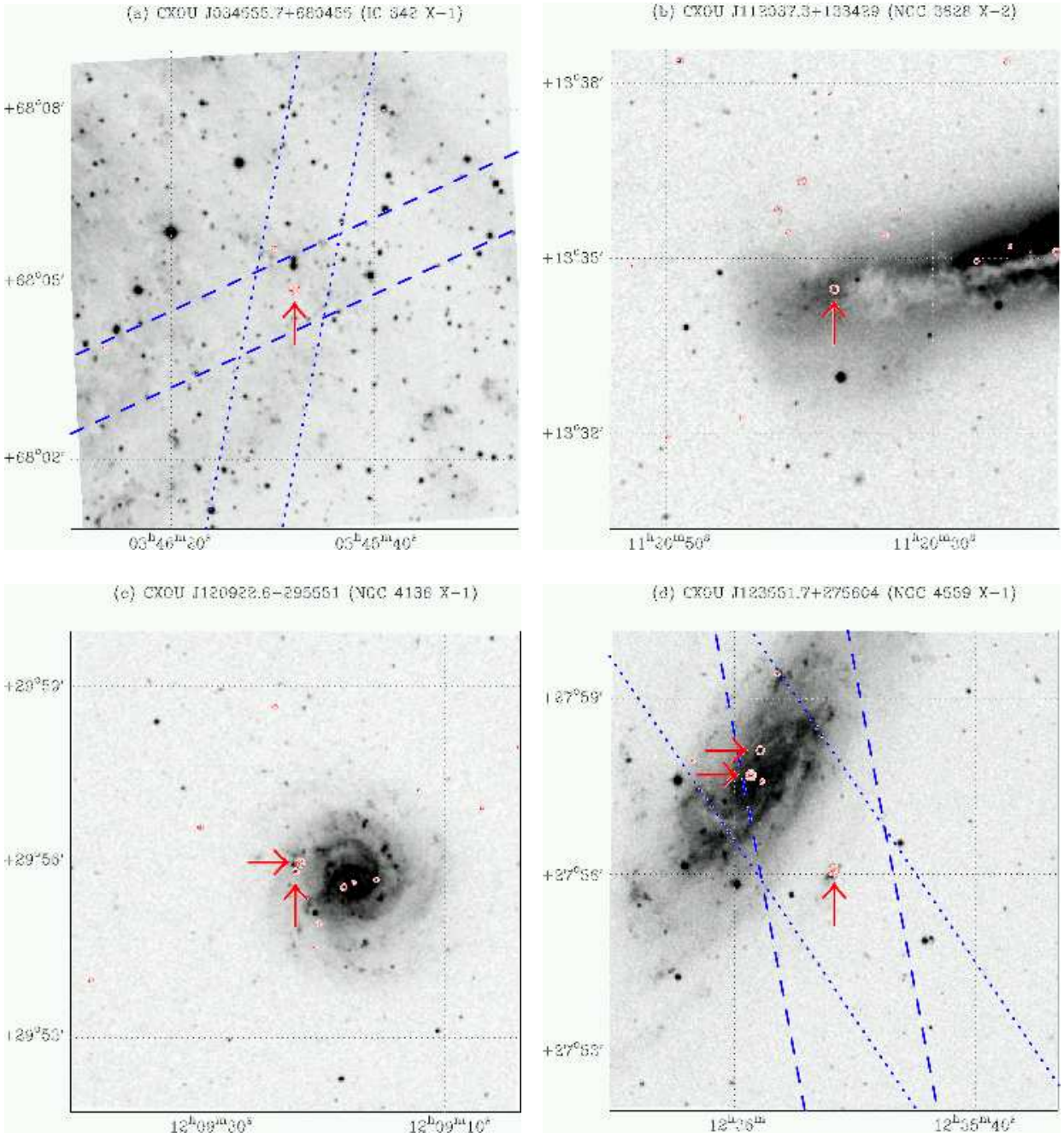

Figure 1. The locations of four of the five target ULXs. Each figure shows an $8.1' \times 8.1'$ DSS-2 blue image centred on the position of the ULX, rotated slightly to match the *Chandra* projection. Coordinates are shown in J2000. The *Chandra* X-ray emission contours are overlayed in red to highlight the positions of the X-ray sources in each field-of-view. The *Chandra* data has been smoothed by a HWHM 3 pixel Gaussian mask to aid visibility, and the contours are plotted at 0.3 and 10 count pixel^{-1}. The target ULXs are highlighted by the vertical arrows, and the field ULXs by horizontal arrows. The spatial coverage of the *Chandra* sub-arrays used for observations of the IC 342 X-1 and NGC 4559 X-1 fields are highlighted in blue for each respective field, with the first epoch coverage shown by the dashed lines, and the second epoch by the dotted lines.

tool[3]. The spectra were grouped to a minimum of 20 counts per bin, and then analysed in XSPEC v.11.2, excluding data below 0.5 keV due to the uncertainty in the calibration at these energies. In the following analysis, all quoted errors are the 90% confidence errors for one interesting parameter.

A major consideration in the design of these observations was to limit the distorting effect of detector pile-up on the observed X-ray spectrum of each ULX. As stated in Section 2, the *ROSAT* HRI count rates of each ULX were used to determine the optimum sub-array size to lower the anticipated pile-up fraction below 10%. However, this did not guarantee that each source would have an acceptable level of pile-up, due to the long-term variable nature of the ULXs themselves (see below). We can derive a lower limit on the observed pile-up fraction of each observation by reference to

[3] See `http://asc.harvard.edu/cal/Acis/Cal_prods/qeDeg`.

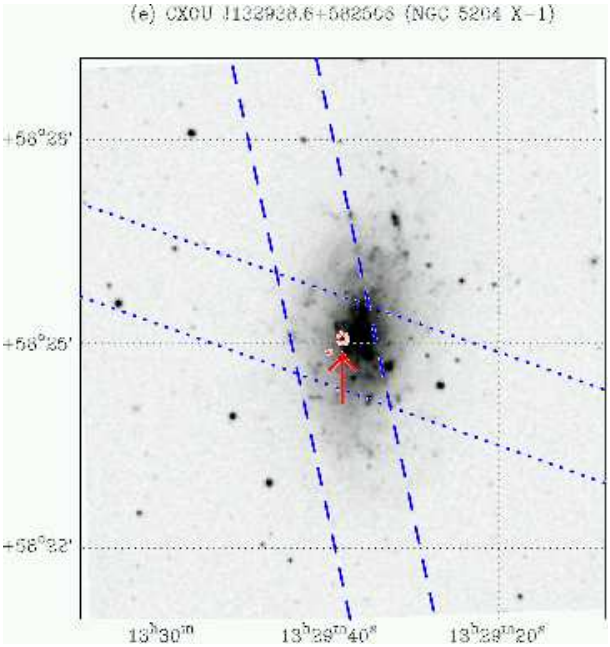

Figure 2. As per figure 1, for the NGC 5204 X-1 field.

Figure 6.24 of the *Chandra* Proposer's Observatory Guide (v.4)[4], which shows pile-up fraction as a function of counts per readout frame (we calculate a lower limit since our input is the *observed* counts per frame, which already includes piled-up events). This is very much a first order approximation, since it does not include, for example, the effect of variations in the source spectra on the degree of pile-up. Only one observation, the 2001 January observation of CXOU J132938.6+582506, turns out to have a lower limit in excess of 10%, and this is only marginal at 11%. All other observations have limits of 8% pile-up or less, implying that the policy of using sub-arrays was successful.

We investigated the presence of residual pile-up effects using the XSPEC v.11.2 parameterisation of the CCD event pile-up model of Davis (2001). A simple absorbed powerlaw continuum model, both with and without the pile-up model, was fit to the observed spectrum of the brightest ULXs (namely CXOU J132938.6+582506, CXOU J123551.7+275604 and CXOU J034555.7+680455 in both epochs, and CXOU J123558.6+275742 in its second observational epoch). In the pile-up model we allowed α, the grade morphing parameter, to vary freely, and set the frame time to 0.7 seconds and 1.1 seconds for the $\frac{1}{8}$ and $\frac{1}{4}$ sub-arrays respectively, with the other parameters fixed as default. In six of the seven cases the changes to the spectral fit when the pile-up algorithm was applied were minimal ($\Delta\chi^2 < 3$ for one extra degree of freedom). Though in most cases the powerlaw photon indices became slightly softer, as expected since CCD pile-up acts to harden the observed source spectra, this change was offset by much worse constraints on the parameters. Hence, the absorption columns and powerlaw photon indices were consistent both with and without the inclusion of the pile-up model, within the derived errors, in all six cases. None of these six fits were able to place strong constraints on α. We therefore consider pile-up effects to be negligible in the X-ray spectra of all but one of the ULXs.

The only case in which the pile-up model gave a much improved χ^2 was the 2001 January observation of CXOU J132938.6+582506, with $\Delta\chi^2 = 16.3$ for one extra degree of freedom, and a statistically significant softening of the spectral slope. We discuss this case further below.

The ULX observations in which less than 250 source counts were accumulated were not considered for spectral analysis, which ruled out both observations of CXOU J120922.6+295551 and CXOU J123557.8+275807. The remaining spectra were initially fit with simple absorbed single component spectral models, namely a powerlaw continuum, a thermal bremsstrahlung model, the multi-colour disc blackbody model (hereafter MCDBB) used to describe an accretion disc around a black hole in its high (soft) state (Mitsuda et al. 1984), a MEKAL optically thin thermal plasma model, and a conventional blackbody spectrum. The best-fit parameters to the powerlaw continuum and MCDBB models are listed in Table 4, and individual cases are discussed below. The thermal bremsstrahlung model provided an adequate fit in most cases, though never as statistically acceptable as a powerlaw continuum (or MCDBB in the case of CXOU J123558.6+275742). We omit it from the table in favour of the two models that have more generally been used to describe ULX spectra in past analyses. The spectra were generally too hard to provide meaningful fits to the MEKAL model, whose parameters tended towards those of the thermal bremsstrahlung fit. Similarly, simple blackbody models did not provide a good fit to any of the spectra.

As shown in Table 4, most datasets are adequately described by a single (absorbed) spectral model component, with a reduced-χ^2 value at, or below, unity. However, in several instances the reduced-χ^2 is still considerably above one. We have attempted to fit these datasets with more complex two-component models (see Table 5). All three datasets for which the spectral fit was improved by the addition of a second spectral component (excluding the pile-up correction to CXOU J132938.6+582506) required the presence of a very soft spectral component. These are discussed on a case-by-case basis in the following sub-sections, where we discuss the spectral fits to each individual ULX. We demonstrate the spectral

[4] See `http://asc.harvard.edu/proposer/POG/index.html`.

Table 4. Best fits of two simple models to the two-epoch ULX X-ray spectra.

ULX (CXOU J)	Epoch	WA*PO[a]			WA*DISKBB[a]			L_X[b]
		N_H[c]	Γ[d]	χ^2/dof	N_H[c]	kT_{in}[e]	χ^2/dof	
034555.7+680455	2002-04-29	0.52 ± 0.07	$1.63^{+0.13}_{-0.12}$	**78.8/81**	$0.30^{+0.05}_{-0.04}$	$1.81^{+0.22}_{-0.18}$	97.4/81	4.4(5.9)
	2002-08-26	0.61 ± 0.08	$1.70^{+0.12}_{-0.13}$	**92.0/87**	0.36 ± 0.05	$1.76^{+0.19}_{-0.16}$	105.7/87	4.4(6.4)
112037.3+133429	2002-04-06	0.022^f	1.57 ± 0.24	**8.4/10**	0.022^f	$0.95^{+0.3}_{-0.2}$	12.3/10	0.7(0.8)
	2002-07-04	$0.16^{+0.09}_{-0.13}$	$2.20^{+0.34}_{-0.19}$	**4.4/10**	0.022^f	$0.86^{+0.18}_{-0.14}$	6.4/11	0.6(0.7)
120922.2+295600	2002-03-07	$0.13^{+0.08}_{-0.07}$	$1.68^{+0.27}_{-0.22}$	**30.1/19**	0.016^f	$1.46^{+0.27}_{-0.25}$	37.7/20	2.3(2.6)
	2002-06-08	< 0.21	$1.55^{+0.30}_{-0.33}$	**13.9/13**	0.016^f	$1.43^{+0.44}_{-0.24}$	18.4/14	1.7(1.9)
123551.7+275604	2001-01-14	0.015^f	1.91 ± 0.09	**69.9/52**	0.015^f	$[\sim 0.84]^g$	169/52	9.8(10.0)
	2001-06-04	0.04 ± 0.03	$2.16^{+0.15}_{-0.14}$	**100/72**	0.015^f	$[\sim 0.66]^g$	222/73	11.6(12.5)
123558.6+275742	2001-01-14	$0.17^{+0.08}_{-0.07}$	$1.98^{+0.23}_{-0.24}$	26.3/22	0.015^f	$1.14^{+0.15}_{-0.13}$	**24.6/23**	4.2(4.3)
	2001-06-04	0.16 ± 0.06	$1.82^{+0.17}_{-0.15}$	63.6/51	0.015^f	$1.30^{+0.12}_{-0.10}$	**49.2/52**	8.9(9.1)
132938.6+582506	2001-01-09	0.10 ± 0.02	$2.38^{+0.10}_{-0.11}$	**141/109**	0.014^f	$[\sim 0.7]^g$	260/110	5.7(6.9)
	2001-05-02	$0.10^{+0.05}_{-0.04}$	$2.96^{+0.25}_{-0.21}$	**41.1/46**	0.014^f	$0.44^{+0.04}_{-0.03}$	86.5/47	1.8(2.4)

Notes: [a]Spectral model components are shown as per the XSPEC syntax, with "WA" representing a cold absorption model, "PO" a powerlaw continuum and "DISKBB" the MCDBB model. [b]Observed luminosity in the 0.5 – 8 keV band in units of 10^{39} erg s^{-1}. Figures in parentheses give the intrinsic (unabsorbed) luminosity. We calculate these values using the best-fitting model highlighted by showing its χ^2/dof in bold. [c]Absorption column, in units of 10^{22} atoms cm^{-2}. [d]Powerlaw photon index. [e]Inner accretion disc temperature in keV. [f]Value fixed at the foreground Galactic absorption column (see Table 2). [g]Parameter value not constrained by model fit.

Table 5. Two-component fits to the ULX X-ray spectra.

ULX (CXOU J)	Epoch	Model[a]	α	N_H	kT/kT_{in}	Γ	χ^2/dof	$\Delta\chi^{2b}$
120922.2+295600	2002-03-07	WA*(DISKBB+PO)	-	$0.81^{+0.37}_{-0.34}$	$0.12^{+0.05}_{-0.04}$	$1.77^{+0.36}_{-0.34}$	16.7/17	13.4
123551.7+275604	2001-01-14	WA*(DISKBB+PO)	-	< 0.25	$0.20^{+0.15}_{-0.07}$	$1.71^{+0.23}_{-0.16}$	65.0/49	4.9
	2001-06-04	WA*(DISKBB+PO)	-	$0.19^{+0.08}_{-0.14}$	$0.15^{+0.10}_{-0.03}$	$2.10^{+0.18}_{-0.26}$	92.4/70	7.6
		WA*(MEKAL+PO)	-	$0.41^{+0.13}_{-0.19}$	$0.18^{+0.05}_{-0.02}$	$2.34^{+0.10}_{-0.14}$	76.7/70	23.3
132938.6+582506	2001-01-09	PILEUP*WA*PO	$0.57^{+0.32}_{-0.18}$	0.14 ± 0.03	-	$2.79^{+0.16}_{-0.14}$	124/108	16.3

Note: [a]The model components and parameters are as per Table 4, except for the MEKAL component which is a thermal plasma model with its metallicity fixed at solar abundance, and PILEUP which is as described in the text. [b]Improvement in the χ^2 statistic over the single component model best-fit, for two extra degrees of freedom (one extra in the pile-up model).

quality of each observation of each source in Figures 3 and 4. These show the data and the best-fit single component model in the upper window of each panel, and the residuals when the data is divided by the best-fitting model in the lower panel.

4.2.1 CXOU J034555.7+680455 (IC 342 X-1)

This ULX showed a fairly constant X-ray spectrum between the two observations, with an absorbed powerlaw continuum providing a good fit to the data from both epochs. In each case the absorption was roughly twice the foreground value (c.f. Table 2), with the additional absorption of $2 - 3 \times 10^{21}$ atoms cm^{-2} in excess of the integrated column through IC 342 at the ULX position ($\sim 8 \times 10^{20}$ atoms cm^{-2}; Crosthwaite, Turner & Ho 2000). This implies a source of additional absorption intrinsic to, or in the environment of, CXOU J034555.7+680455. This may originate in the nebula surrounding this ULX described by Roberts et al. (2003). The *Chandra* spectra are consistent with the low/hard spectral state observed by *ASCA* in 2000 February 24 - March 1, described by an absorbed powerlaw continuum with $N_H = 0.64 \pm 0.07 \times 10^{22}$ atoms cm^{-2} and $\Gamma = 1.73 \pm 0.06$ (Kubota et al. 2001). This state has also been interpreted as an anomalous/very high state (Kubota, Done & Makishima 2002), which we discuss further in Section 5.1. The luminosity also appears little changed, at $\sim 5 \times 10^{39}$ erg s^{-1} (versus 6×10^{39} erg s^{-1} in *ASCA*) when extrapolated to the 0.5 – 10 keV band. Hence it appears that this ULX has been in a constant spectral state in three separate observations over 2.5 years.

4.2.2 CXOU J112037.3+133429 (NGC 3628 X-2)

This ULX had faded to a luminosity of only $\sim 7 \times 10^{38}$ erg s^{-1} in our *Chandra* observations, hence the spectra are of low quality, and the spectral models were not strongly constrained. A powerlaw continuum was again the preferred model in both epochs, though the MCDBB also gave a statistically-acceptable fit in the second epoch. The source flux appeared to change little between the epochs, perhaps fading slightly in the three months between observations. However, despite the low quality, the intrinsic X-ray spectrum showed changes between the epochs, with the first observation showing an intrinsically hard ($\Gamma \sim 1.57$) but unobscured powerlaw continuum, whereas the second observation showed a softer intrinsic slope ($\Gamma \sim 2.2$) with a low-energy turnover due to absorption.

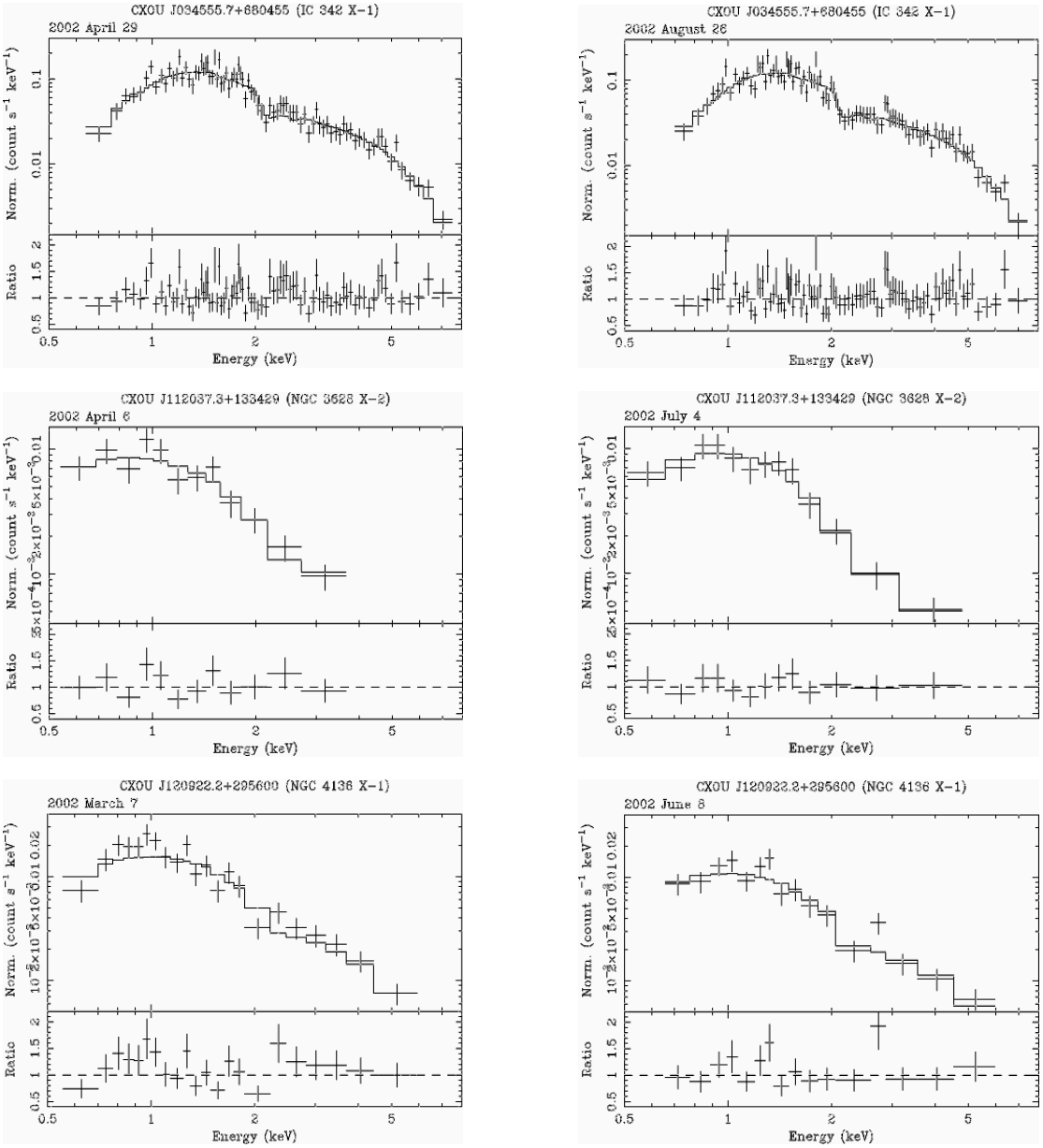

Figure 3. The *Chandra* ACIS-S3 spectra of the ULXs. We show the data and best-fit single component model in the top window of each panel, and the ratio of the data to the model in the lower window. We plot the first and second epoch data for each ULX in the left and right columns respectively, using the same normalisation scaling for each pair of spectra to aid their direct comparison. All spectra are shown using the same energy scale, and the ratio values are all displayed over the same range.

4.2.3 CXOU J120922.2+295600

This new ULX has a spectrum which is best-fit by a powerlaw continuum model in both epochs. However, the powerlaw fit is only statistically-acceptable in the second epoch. In order to improve the fit to the first epoch data we tried a variety of two-component spectral fits to the data. The best fits came from models with a highly absorbed, very soft component in addition to a hard powerlaw continuum. We show such a fit, with the very soft component modelled by a MCDBB, in Table 5. This fit is statistically acceptable for the data, and an improvement over the single powerlaw continuum model at 99.97% ($> 3\sigma$) confidence. Note, however, that the addition of a classical blackbody emission model (with $kT = 0.1$ keV) rather than a MCDBB model provides an equally acceptable fit to the data. The powerlaw continuum slope is consistent (within the large errors) in both epochs, though the inferred absorption column is much lower in the absence of a very soft component in the second observation.

4.2.4 CXOU J123551.7+275604 (NGC 4559 X-1)

This is the most luminous ULX in the sample, with its observed luminosity at, or above, 10^{40} erg s^{-1}. Its X-ray spectrum was observed to soften between the observations, with the X-ray emission in the second, more X-ray luminous epoch represented by a significantly softer powerlaw photon index than the first (~ 2.16 against ~ 1.91). However, its X-ray spectrum is not well-fit by either simple model, with the MCDBB model rejected at high sta-

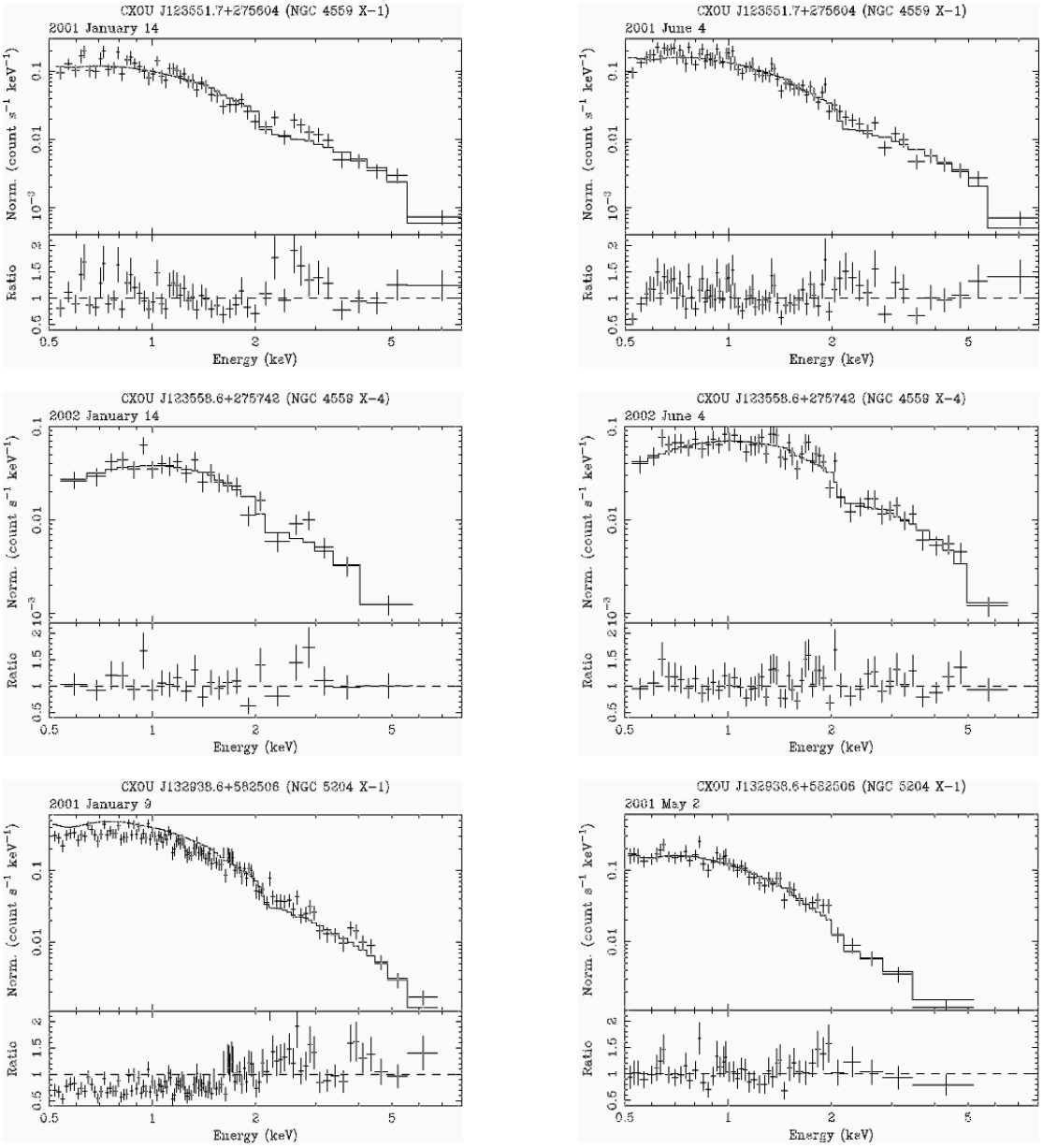

Figure 4. As for Figure 3, except for the first epoch spectrum of CXOU J132938.6+582506. Here we plot the pile-up corrected spectral model over the actual data, to demonstrate the degree of pile-up in the observed X-ray spectrum.

tistical significance. Two-component models incorporating a very soft MCDBB plus a powerlaw continuum offered improvements to the fit, as shown in Table 5, though only at the 69% and 94% significance levels in the first and second epochs respectively. A classic blackbody component offered a superior improvement in the second epoch, at the 96% significance level according to the F-statistic.

Curiously, a substantial improvement in the fit to the second epoch data was obtained when the MCDBB component was replaced with a MEKAL solar abundance thermal plasma with $kT \sim 0.18$ keV (Table 5). For two additional free parameters, the reduction in χ^2 of 23.3 implies a 99.99% significance level (i.e. $> 3.5\sigma$) in terms of the F-test. Figure 5 shows the resulting best-fit spectrum and the contribution of the MEKAL component. For comparison, a similar model (powerlaw plus $kT \sim 0.18$ keV MEKAL) was fitted to the first-epoch data and no significant improvement to the best-fit was obtained, with the contribution of the putative thermal component limited to no more than 3% of the 0.5 – 8 keV flux.

However, the MEKAL fit relies heavily on the fact that a blend of lines between 0.5 – 0.75 keV (predominantly OVII and OVIII), when combined with a factor ~ 2 increase in the model N_H, gives a good match to the additional soft emission apparent in the second-epoch spectrum. Is this thermal component real or simply an artefact of fitting a fairly complex model to data with limited spectral resolution and poor statistics (N.B. ~ 600 counts out of ~ 2000 in the full spectrum originate from the MEKAL component)? Clearly there is no direct evidence in the second-epoch spectrum for individual lines (though this is perhaps consistent with low temperature of the plasma and the > 100 eV spectral resolution of the ACIS-S detector below 1 keV). On the other hand when we allow the abundance of O, Ne and Fe (which produce the most significant line features in the $kT \sim 0.18$ keV plasma) to vary in the VMEKAL

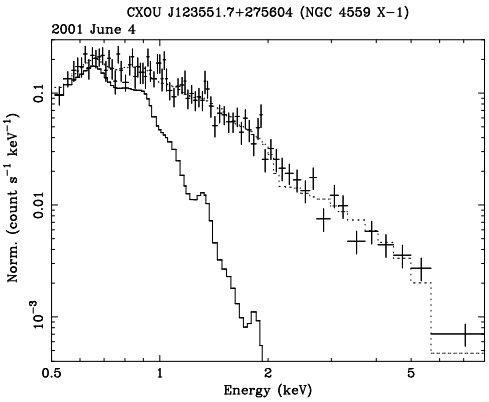

Figure 5. The second epoch count rate spectrum of CXOU J123551.7+275604. The best-fit of the powerlaw plus MEKAL model to the overall spectrum is shown as the dotted line with the contribution of the MEKAL component highlighted (solid line).

model, we obtain a best-fit of 1.3 solar and a 90% lower-limit of 0.33 solar, implying that there is a strong preference for a substantial contribution from emission lines. *However, this is on the basis of a spectral model which may not be correct*. We conclude that an interpretation of the additional soft flux present in the second-epoch in terms of the emergence of a bright thermal component is potentially very interesting (see Section 5.3), albeit highly speculative.

Finally, we note that as this paper was undergoing the refereeing process these *Chandra* spectra were published by Cropper et al. (2003) as part of an *XMM-Newton* study of this source. They do not report the possible detection of a MEKAL component, though they did not explicitly look for it. Instead they fit a particular model to the *Chandra* data, based on fits to the superior quality (and later epoch) *XMM-Newton* spectra, comprising a sub-solar abundance absorber (TBVARABS, set at 0.31 times solar) applied to powerlaw plus blackbody emission components. We have applied the Cropper et al. model, plus variants incorporating soft MCDBB and MEKAL components, to the second-epoch spectrum and do get a marginal improvement in each case with respect to our original fits ($\Delta\chi^2 \sim 2-4$); nevertheless the powerlaw plus MEKAL model still clearly provides the best result in terms of the minimum χ^2.

4.2.5 CXOU J123558.6+275742 (NGC 4559 X-4)

This object was the only ULX in the sample with an X-ray spectrum clearly best-fit with a MCDBB model. The inferred inner accretion disc temperatures were both greater than 1 keV, consistent with previous *ASCA*, and some *Chandra* observations of ULX well-fit by this model (e.g. Colbert & Mushotzky 1999; Makishima et al. 2000; Roberts et al. 2002). The luminosity of the ULX more than doubles in the five months between observations, and this is associated with a slight hardening of the X-ray spectrum, with the best-fit temperature of the inner accretion disc rising from ~ 1.1 to ~ 1.3 keV.

4.2.6 CXOU J132938.6+582506 (NGC 5204 X-1)

The X-ray spectrum of this ULX was far better fit by a powerlaw continuum model than a MCDBB in both epochs, with it constituting a statistically-acceptable fit in the second epoch. It was a poorer fit in the first epoch, though this observation was affected by a pile-up fraction of in excess of 10% of all events (see above). The XSPEC v.11.2 parameterisation of the Davis (2001) pile-up correction model was used to correct for this effect, the results of which are shown in Table 5. This resulted in a much improved fit to a powerlaw continuum spectrum, with the inferred photon index softening considerably. Hence, whilst the two uncorrected spectra appear to have very different hardnesses, after the correction for pile-up they are both revealed to be intrinsically very soft X-ray spectra. The photon indices of the powerlaw continuum fits are consistent within the errors after pile-up correction, albeit with a slightly harder value in the far more luminous first observation.

4.3 Temporal properties

4.3.1 Short-term variability

We derived short-term lightcurves for seven of the eight ULXs in both of their observation epochs, using the CIAO routine LIGHTCURVE. The exception was CXOU J120922.6+295551, which was too faint for this analysis with only 59 and 90 counts detected in total per epoch. Each lightcurve was binned to an average (over the observation) of 25 counts per bin, giving temporal resolutions ranging from ~ 60 seconds in the best case, to ~ 2500 seconds. The resulting data was tested for gross variability using a χ^2 test against the hypothesis of a constant count rate. Five of the ULX showed no strong evidence for short-term temporal variability in either epoch, with a reduced-χ^2 statistic of 1.25 or less. However, two ULX showed strong evidence for short-term variability in one of their two observation epochs. These lightcurves are plotted in Figure 6. The appropriate χ^2/degrees of freedom statistics are 39.5/14 for the 2002 June observation of CXO J120922.2+295600 (which had a 1407 second resolution), and 190/24 for CXOU J123558.6+275742 in its 2001 January observation (at 404 second resolution). The other observations of both sources were consistent with a constant flux, implying that the short-term variability states are themselves a transient phenomenon. These highly-variable states both occur when the ULX in question is (on average) at the lower of its two observed X-ray fluxes.

We also performed a Kolmogorov-Smirnov test comparing the cumulative photon arrival times with the expected arrival times, assuming each source flux was invariant with time. This provides a separate indicator of short-term variability, free of any possible gross binning effects, and sensitive to lower-amplitude (10 – 20%) sustained changes in the ULX count rates than the χ^2 test. We performed this test on all eight ULXs. It confirmed that the 2002 June observation of CXO J120922.2+295600 was variable at $> 99\%$ probability. Curiously, the 2001 January observation of CXOU J123558.6+275742 was only variable at the $\sim 90\%$ level according to the Kolmogorov-Smirnov test. Again, none of the other ULX appeared variable according to this test.

In the January 2001 lightcurve of CXOU J123558.6+275742 there are four "peaks" in the X-ray emission, separated by regular intervals of 6 – 7 bins, during which the X-ray flux is 4 – 5 times brighter than in the lowest flux bins. This hints at a possible characteristic timescale for the variability of ~ 2500 seconds for the peaks. It is also noticeable that the lightcurve behaves similarly between the peaks (this quasi-repetitive behaviour is the likely reason for the lower probability of this source being variable according to the Kolmogorov-Smirnov test). Similar regular variability in the form of "quasi-periodic flaring" has recently been revealed in three separate observations of an extremely variable ULX in M74, CXO J013651.1+154547 (Krauss et al. 2003). However, the characteris-

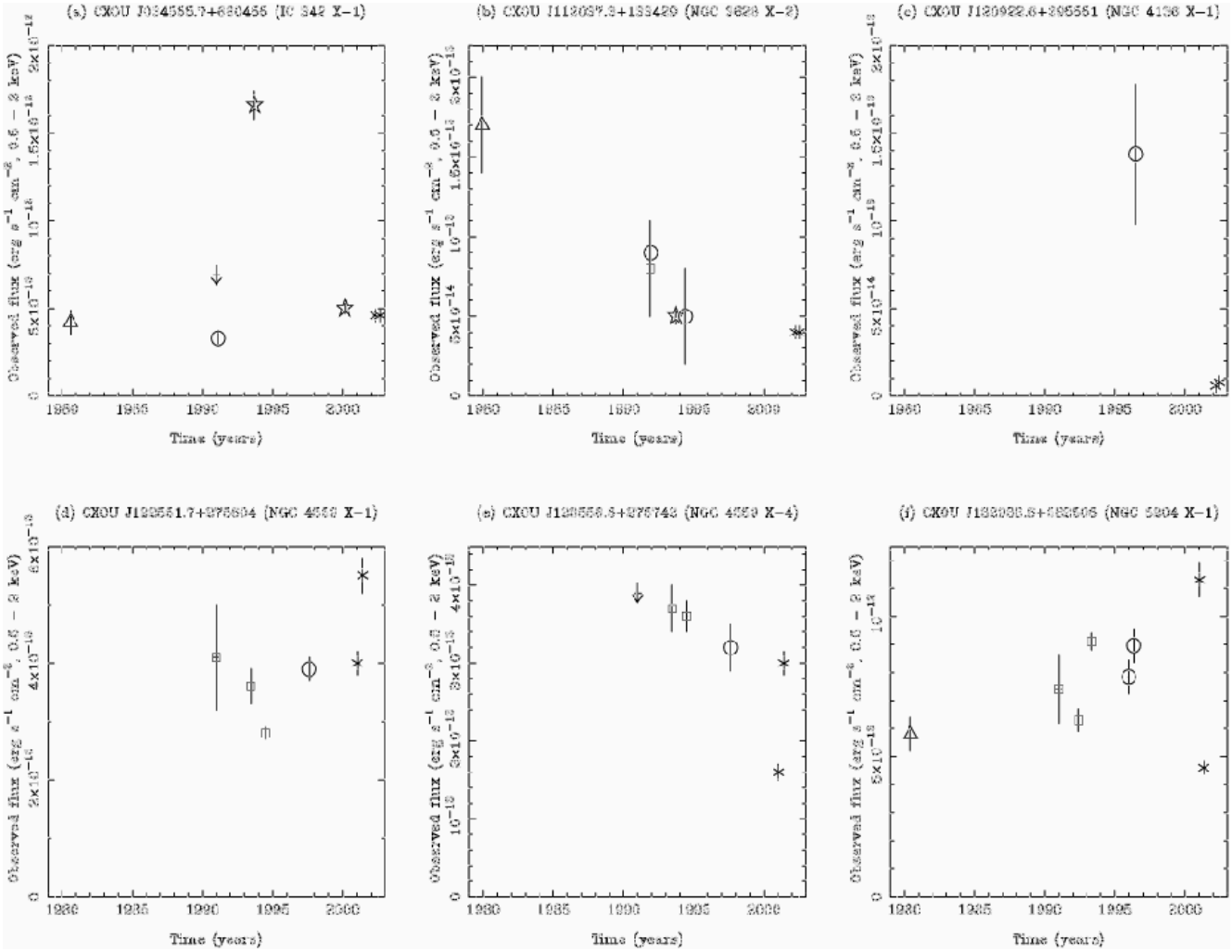

Figure 7. Long-term lightcurves for six of the ULXs. The data points shown originate from *Einstein* IPC (triangles), *ROSAT* PSPC (squares), *ROSAT* HRI (circles), *ASCA* (stars) and *Chandra* (asterisks) measurements, which have been converted to a 0.5 – 2 keV flux as described in the text. Each panel is normalised independently to highlight the variability of each ULX.

tic timescales of these variations are somewhat longer, inferred to be at $\sim 3600 - 7900$ seconds, and the flares have a larger amplitude, reaching more than an order of magnitude brighter than the quiescent level for this ULX. Claims of actual periodic variations have so far only been made for three ULXs. A period of 7620 ± 500 seconds was reported for a bright state of the ULX M51 X-7 (Liu et al. 2003), albeit on the basis of a 15 ks observation. A 7.5 hr period was derived for a ULX coincident with the Circinus galaxy (Bauer et al. 2001), though given the proximity of Circinus to the Galactic plane and the similarity of the periodicity to a long-period AM Her system it is possible that this source is a foreground interloper. The only other apparently periodic variations in an ULX were reported by Sugiho et al. (2001) for IC 342 source 3, but these were very small amplitude ($\sim 5\%$) and on a timescale of 30 – 40 hours.

4.3.2 Long-term variability

Six of the eight ULXs have been detected and catalogued in the data from previous X-ray observatories. The long-term variability lightcurves for these objects are plotted in Figure 7, using data from the *Einstein*, *ROSAT* and *ASCA* observatories in addition to our new *Chandra* data. Each lightcurve is plotted in terms of the observed 0.5 – 2 keV flux of the ULX, with this particular band chosen for its commonality between the missions. The flux is either directly measured from our best fit spectral models, in the case of the *Chandra* data, or is a flux quoted from previous spectral measurements of the source in question (using *ASCA* and some *ROSAT* PSPC data: see Appendix A for references), or are calculated from the observed count rates or fluxes given in a wider band. In the latter cases, we assume spectral models that are coarse averages of the two *Chandra* observations (e.g. an absorbed powerlaw continuum model with $\Gamma = 2$ and $N_H = 2 \times 10^{20}$ atoms cm^{-2} for CXOU J123551.7+275604), and use either PIMMS or XSPEC to normalise the observed count rate into an observed 0.5 – 2 keV flux. Finally, we correct the *Einstein* and *ASCA* count rates of CXOU J112037.3+133429 for confusion with the two moderately-bright sources immediately to its north-northwest (c.f. Figure 1), and we similarly correct the *ROSAT* PSPC data for CXOU J123558.6+275742 for confusion with other sources in proximity to the nucleus of NGC 4559, both on the basis of the *Chandra* observations.

The long-term lightcurves of the ULXs are obviously very

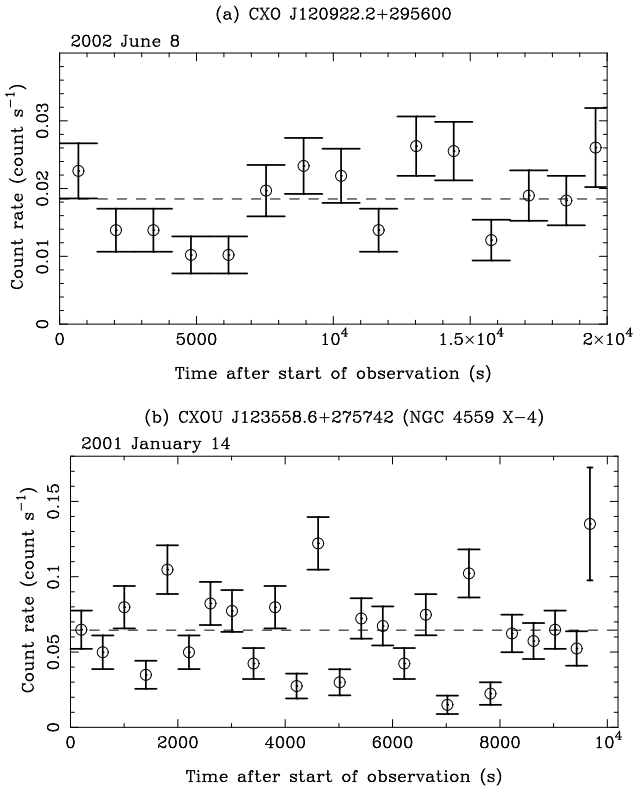

Figure 6. The short-term variability observed in two ULXs. The data in both panels is binned such that, at the mean count rate (shown by the dashed line) each temporal bin would contain 25 counts.

poorly sampled, with between three and eight observations, each typically only a few hours long, covering a baseline from 6 to 23 years. However, despite the low quality, there does appear to be some variety evident in the behaviour of the different ULX. Two sources - CXOU J123551.7+275604 and CXOU J132938.6+582506 - appear to have varied quite randomly over their observational histories, with a maximum change in their observed flux of little more than a factor of two. On the other hand, the average flux of CXOU J112037.3+133429 appears to have consistently decayed over 23 years of observations to $\sim$ 25% of the value inferred from the *Einstein* IPC. A possible decay is also observed from CXOU J123558.6+275742, with the exception of a large dip in its first *Chandra* epoch, which coincides with the epoch of extreme short-term variability in this ULX. A further source whose flux has decayed since its initial detection is CXOU J120922.6+295551, which has faded by a factor $\sim$ 20 over the six years between its initial detection in a *ROSAT* HRI image and the current *Chandra* observations. Finally, CXOU J034555.7+680455 appears at around the same 0.5 – 2 keV flux ($4 \pm 1 \times 10^{-13}$ erg cm^{-2} s^{-1}) in all but one of its observations. The exception is the 1993 September observation in which it displayed a high/soft spectral state, with an average flux four times higher than in other epochs. This may indicate that the high/soft state is rare in this source.

We do not present long-term lightcurves for the two previously undetected ULXs. The 0.5 – 2 keV flux of CXOU J120922.2+295600 in the *Chandra* observations was $\sim 5 - 7 \times 10^{-14}$ erg cm^{-2} s^{-1}; if this flux was the same during the previous *ROSAT* HRI observation of this galaxy, it would have remained undetected (NGC 4136 X-1 $\equiv$ CXOU J120922.6+295551 was a marginal detection at $\sim 1.5 \times 10^{-13}$ erg cm^{-2} s^{-1}). On the other hand, CXOU J123557.8+275807 was observed to have a flux of $3-6 \times 10^{-14}$ erg cm^{-2} s^{-1} in the *Chandra* observations, which compares to detection limits of around 1 and 4×10^{-14} erg cm^{-2} s^{-1} in the *ROSAT* PSPC and HRI observations of NGC 4559 respectively. This implies that this ULX is possibly a transient source.

Finally, our *Chandra* observations reveal that two out of the five target ULXs have faded to X-ray luminosities that are below the arbitrary limit of 10^{39} erg s^{-1} that we use to demarcate the ULX population from the "normal" X-ray source population in nearby galaxies. An important aim for future studies will be to determine how common this behaviour is for ULXs, and in particular to define their duty cycle, allowing us to estimate the true number of potential ULXs in nearby galaxies.

5 DISCUSSION: CLUES TO THE NATURE OF ULXS FROM THEIR BEHAVIOUR?

5.1 Similar behaviour

Are there any general trends revealed in our data that can help cast light on the nature of ULXs? Several similarities across the sample are highlighted by the analysis in the previous sections. They are all spatially consistent with point-like sources, and when their ubiquitous long-term variability (and in some cases extreme short-term variability) is considered it is very likely that their X-ray emission originates in a single X-ray emitting system. The majority of the best-fit X-ray spectral models show an absorption column well in excess of that along the line-of-sight to each ULX through our own galaxy. This may either be an additional column through the host galaxy, or perhaps material intrinsic to the ULX itself. The lack of variation in the absorption column where it is constrained by the same physical model at both epochs (c.f. Table 4) suggests that it may not originate in the very close proximity of the ULX, although it may still be associated with gas and dust in their immediate environment.

It is likely that the majority of the ULXs are associated with the young stellar populations of the active star formation regions in their host galaxies. The issue of whether this implies that they do not contain an IMBH primary remains controversial. Models for IMBH formation in young, dense stellar clusters (e.g. Ebisuzaki et al. 2001; Portegies-Zwart & McMillan 2002) certainly argue that star formation regions could host IMBHs, though the observed displacement between stellar clusters and ULX positions in the Antennae (Zezas et al. 2002) argues that at least in this case many of these ULXs are runaway binaries (i.e. ordinary X-ray binaries kicked out of the stellar clusters by the supernova explosions that formed the compact primary). If alternately the IMBHs were formed before the current epoch of star formation, for instance as the remnants of the primordial Population III stars (Madau & Rees 2001), it is unlikely that they could accrete sufficient material to appear ULX-bright even in the gas-rich environment of star-formation regions (c.f. Miller & Hamilton 2002), therefore they are reliant upon capturing a secondary star to accrete from. The chances of this occurring could be higher within the dense stellar environments of star forming regions. However, whatever the origin of the IMBH, King (2003b) argues that extremely large underlying populations of these objects are required in order to account for the numbers of ULXs observed in the brightest starburst galaxies such as the Cartwheel galaxy (c.f. Gao et al. 2003). This strongly argues that ULXs associated with star formation are, as a class, dominated by "ordinary"

HMXBs that somehow exceed their Eddington limit. The likely association of the ULXs in our sample with young stellar populations could simply be the extension of the ULX – star formation relationship into lower star-formation rate "normal" spiral galaxies. If so, then it is likely that our objects may also be predominantly HMXBs.

Next, *Chandra* does not detect extreme short-term X-ray variability (on the scale of hundreds of seconds over a baseline of three to six hours) as a common feature of these ULXs - it is only present in two of 14 observations - implying that in the majority of ULX states either the X-ray emission is reasonably constant, or it varies on much shorter timescales than we have sampled. The absence of extreme short-term variability, on the basis of *Chandra* observations, has also been noted for many other ULXs in spiral galaxies (c.f. Strickland et al. 2001; Roberts et al. 2002), The lack of this behaviour in the majority of ULXs argues strongly against the relativistic beaming model as the dominant emission mechanism for ULXs, since presumably this would require a remarkably stable jet to avoid large amplitude flux variation, due to both its narrow beam angle and the strong amplification of any variations via Doppler boosting.

On the other hand, the absence of extreme long-term variability is also interesting, with most of the ULXs seen to vary only by factors of up to ~ 4 over periods of up to twenty years. This suggests that they are all persistent X-ray sources, rather than short duty-cycle transients. Interestingly, a comparison with the 18 dynamically-confirmed Galactic black hole binaries shows that the only persistent sources over the last ~ 30 years are the three HMXBs (McClintock & Remillard 2003). Furthermore, observations of one of the HMXBs, Cyg X-1, with RXTE have shown its flux to vary by no more than a factor of ~ 4 over seven years of continuous observations (Pottschmidt et al. 2003). These similarities may be another clue linking ULXs to HMXBs, although whether this is a fair comparison given that the three Galactic HMXB/BH sources are all wind accretors with $\mathrm{L_X}$ well below 10^{39} erg s^{-1} is open to debate.

A further trend revealed by the data analysis is that the X-ray spectra of the ULXs are generally better fit by powerlaw continua than by MCDBB models, with only one out of six ULXs showing a preference for the latter (though we note that in three of the ten powerlaw spectra a combination of low signal-to-noise and a low χ^2/dof value implies that we cannot exclude MCDBB models to a high statistical significance). This appears to contradict previous results, particularly those reported from *ASCA* observations by Makishima et al. (2000), which focussed on ULXs well fit by a MCDBB as possible examples of the high/soft state for accreting 10 - 100 $\mathrm{M_\odot}$ black holes. So if these ULXs are comparable to Galactic sources, but are not in the high/soft state, what state are they in? To answer this question we refer to the recent work by McClintock & Remillard (2003), which provides new definitions of the classic black hole states, with firm observational diagnostics based on the results of more than six years of observations with RXTE. However, since we have neither the photon statistics in the *Chandra* data to derive a power density spectrum, or any information on the X-ray spectrum beyond a maximum of 10 keV, we are reliant solely on the photon indices of the powerlaw continua to provide a state diagnostic. The two states described by McClintock & Remillard (2003) that provide the best candidates for the powerlaw-dominated spectra are the low/hard state (which is related to the emission of radio jets) and the steep powerlaw state (previously known as the very high state), with the distinction in photon indices being that the low/hard state typically has values of $\Gamma \sim 1.5-2$, whereas the steep powerlaw state has values of $\Gamma > 2.4$. Using this distinction, it is clear that only one source (CXOU J132938.6+582506) has a sufficiently steep powerlaw to be in the latter class ($\Gamma \sim 2.8-3.0$), with all the other sources more consistent with the low/hard state. It is also notable that Galactic black holes in the steep powerlaw state tend to have a substantial contribution from a MCDBB component with $kT_{in} \sim 1-2$ keV; we do not see any such composite warm MCDBB + powerlaw continuum spectrum (although the *Chandra* bandpass may not be the optimum choice for recognising such a spectrum).

This provides an observational argument against the suggestion of Kubota, Done & Makishima (2002; see also Terashima & Wilson 2003 for further discussion) that the the powerlaw spectral state of ULXs must be the very high state. Instead, the slopes of the four out of five ULXs best described by powerlaw spectra suggest that the sources are in the low/hard state. Until recently, this would have suggested that the ULX was accreting at a relatively low fraction (maybe $\sim 5\%$) of the Eddington luminosity of the compact object, as black hole states were simplistically assumed to be a function of mass accretion rate (see e.g. Esin, McClintock & Narayan 1997). This would imply black hole masses of $1-2\times10^3$ $\mathrm{M_\odot}$ for these ULXs, i.e. IMBHs. However, it is now clear that the black hole state is not a direct function of mass accretion rate (Homan et al. 2001). This suggests that we cannot rule out observing the low/hard state at or near the Eddington limit for a stellar-mass black hole. However, it is still true that in most known cases the low/hard state occurs well below the Eddington limit, with the one exception being GRS 1915+105 which reaches luminosities $> 10^{38}$ erg s^{-1} in this state (McClintock & Remillard 2003). For ULXs to be low/hard state stellar-mass black hole binaries we would obviously have to rely on some means of boosting the apparent luminosity to explain their super-Eddington fluxes, e.g. anisotropic emission. However, observations of the low/hard state in Galactic black holes have suggested that the accretion disc could be truncated at large distances from the black hole ($\gtrsim 100R_g$), which would present a challenge for models in which the anisotropic emission originates in "funneling" of the radiation by a geometrically-thick inner accretion disc (c.f. King 2003a) (though see McClintock & Remillard 2003 for a discussion of whether the inner disc is truly truncated in the low/hard state). This suggests that the easiest interpretation of this state is that we are observing the low/hard state from accretion onto an IMBH.

The arguments presented above assume that direct analogies to Galactic black hole systems are appropriate for ULXs, when the majority of Galactic black holes spend the majority of their time emitting at far below the 10^{39} erg s^{-1} threshold of ULXs. It is possible then that the hard powerlaw state we are seeing is actually unique to the very high accretion rates required if ULXs are truly the extreme high luminosity end of the stellar-mass black hole population. If this is the case, then super-Eddington ratios (i.e. $\mathrm{L_X/L_{Edd}}$) of up to 10 are required for the ULXs discussed in this paper; this is consistent with the predictions of Begelman (2002) for true super-Eddington discs, and within a factor two of the ratio predicted from simple geometric funelling by Misra & Sriram (2003). Of course, we cannot rule out accretion onto IMBHs as an explanation for the spectra of any of our sources, but it is worth noting that it is now becoming clear that Galactic black holes do show epochs of apparent super-Eddington emission (McClintock & Remillard 2003). Perhaps the most pertinent example of these Galactic sources is GRS 1915+105, which spends a significant fraction of its time emitting at super-Eddington rates for its ~ 14 $\mathrm{M_\odot}$ black hole (Done et al. 2003), and has been in outburst continually

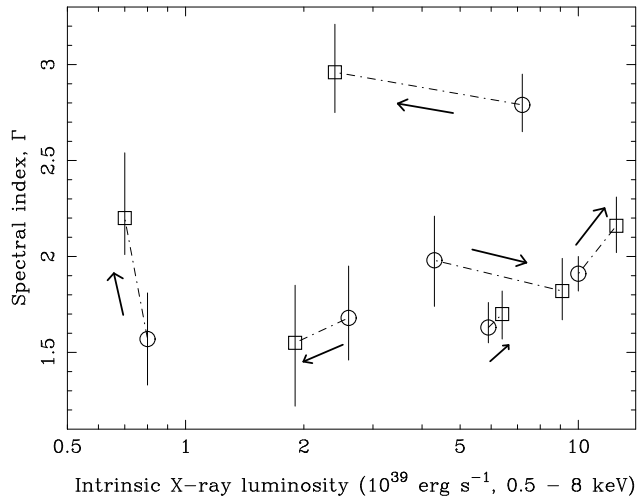

Figure 8. Spectral variability in the ULX as a function of intrinsic X-ray luminosity. The first epoch *Chandra* data is indicated by an open circle, and the second by a square, with the two observations of each source joined by a dot-dash line. The evolution of the photon index with luminosity is highlighted by the arrows, and the errors are the 90% confidence intervals for the spectral parameters.

for the past 11 years. Hence if viewed by an observer outside our galaxy, GRS 1915+105 could frequently appear as a ULX.

5.2 Contrasting behaviour

A remarkable feature of the analysis in the previous sections is the diversity in the observed properties of the ULXs, with the differences between the objects being more pronounced than any similarities. To obtain a deeper understanding of these objects, we adopt a more complete view than simply considering each characteristic in isolation. We approach this by compiling a summary of their observational characteristics in Table 6.

One immediate curiosity highlighted by Table 6 is that the two sources that display short-term variability appear very different. Whilst both the sources are at the lower of their two observed luminosities when variable, their average X-ray spectra during this epoch contrast greatly, with CXOU J120922.2+295600 displaying a hard powerlaw continuum ($\Gamma \sim 1.55$) whereas CXOU J123558.6+275742 has a MCDBB form. The short-term variability and powerlaw spectral form of CXOU J120922.2+295600 may be consistent with its X-ray emission in this state being dominated by a variable, possibly relativistically-beamed jet. However, the thermal accretion disc spectrum of CXOU J123558.6+275742 argues against this interpretation. Further studies of short-term variation in ULXs, based on higher signal-to-noise ratio data, have suggested a number of alternate physical mechanisms including rapid variations in the ULX accretion rate (La Parola et al. 2003), magnetic reconnection events in the accretion disc corona (Roberts & Colbert 2003) and an optically thick outflow (Mukai et al. 2003).

A related issue is the long-term variations in the X-ray spectra of these sources revealed by the *Chandra* data. We note, with reference to Table 4, that all the spectra appear to show changes between the two observational epochs. We summarise these changes in Figure 8 by plotting the best-fit powerlaw photon index for each dataset against the derived intrinsic 0.5 – 8 keV X-ray luminosity for that observation. Though Figure 8 highlights that the 90% confidence intervals for the photon index measurements overlap in almost all cases, consistent with little or no significant change in the photon indices, the best fit values do appear to show some level of variation. The data suggest that three of the ULX spectra are softer in a higher luminosity state, and three are harder. It has been noted elsewhere (e.g. Kubota et al. 2001; La Parola et al. 2001) that some ULX undergo a low/hard to high/soft state transition, reminiscent of the behaviour of classic Galactic black hole X-ray binary systems. Other recent observations have highlighted the opposite behaviour, i.e. a high state in which the spectrum is harder, for instance in M51 X-7 (Liu et al. 2002) and in four out of five ULXs in the Antennae (Fabbiano et al. 2003), one interpretation being that the accretion disc heats up (and hence spectrally hardens) as the luminosity of the system increases. The equal split between "hardening" and "softening" ULXs in our sample suggests that both transitions are common, implying either the ULX population is heterogeneous, with at least two flavours of accretors behaving differently, or that those sources composing the bulk of the ULX population are capable of displaying multiple states and modes of transition between those states.

5.3 (Dis)appearing spectral components

Table 6 also highlights a more spectacular flavour of spectral variation: components that appear to be present at one epoch but not during the other. This occurs in two of the ULXs. In CXOU J120922.2+295600 we see a very soft component, fit by a MCDBB model with $kT_{in} = 0.12$ keV, that is present (though only at 3σ confidence) in the more luminous 2002 March observation but not in 2002 June. A similar soft ($kT < 0.2$ keV) MCDBB component has been reported in other ULX, notably from *XMM-Newton* data for two ULXs in NGC 1313 (Miller et al. 2003), where it is interpreted as spectroscopic evidence for the "cool" accretion disc expected to be present around an IMBH. In CXOU J120922.2+295600 this component disappears in the three-month period between observations. This could be analogous with a classic high/soft to low/hard state transition as seen in Galactic black-hole X-ray binary candidates, but potentially involving an IMBH system in this case. However, there are other potential explanations. Perhaps the best alternative is that the soft component is originating in an optically-thick outflowing photosphere around a black hole X-ray binary, as suggested by Mukai et al. (2003) to account for a highly luminous ultra-soft ULX in M101 (a phenomenon also described as a "black hole wind", see King & Pounds 2003; Fabbiano et al. 2003). Such a component would have a blackbody spectrum with a temperature $kT \sim 0.1$ keV, consistent with the first epoch observation (c.f. section 4.2.3), and might easily switch off between the two observations of the ULX. However, there are arguments against the soft component originating in a black hole wind, most notably in the case of sources that also have a strong hard powerlaw continuum component in their spectrum (e.g. M81 X-9; Miller, Fabian & Miller 2003). In this case the powerlaw component must originate in shocks outside the photosphere, but in order to have comparable luminosity to the soft component Miller et al. argue that the photospheric radius must actually be of the order of the Schwartzschild radius, implying no photosphere for these sources, and hence that the soft component must originate in the accretion disc.

The other ULX to show a changing spectral form was CXOU J123551.7+275604. In this case the spectrum showed a marked softening between the two *Chandra* observations. Earlier we noted that the additional soft flux present in the second-epoch could be modelled in terms of the emergence of soft ($kT = 0.18$ keV)

Table 6. A summary of the ULX characteristics.

ULX (CXOU J)	Epoch	L_X[a]	Variability		Best-fit spectral model[b]	Environment
			Short-term	Long-term		
034555.7+680455	2002-04-29	4.4(5.9)	No	Hard state + soft flare	PL	Spiral arm
	2002-08-26	4.4(6.4)	No			
112037.3+133429	2002-04-06	0.7(0.8)	No	Steady flux decay	PL	Outer disc
	2002-07-04	0.6(0.7)	No			
120922.2+295600	2002-03-07	2.3(2.6)	No	[N/A]	PL + absorbed MCDBB	Spiral arm
	2002-06-08	1.7(1.9)	**Yes**		→ PL	
120922.6+295551	2002-03-07	0.2(0.2)	No	Large drop	[N/A]	Spiral arm
	2002-06-08	0.2(0.2)	No			
123551.7+275604	2001-01-14	9.8(10.0)	No	Random	PL (+ soft component?)	Faint outer spiral arm
	2001-06-04	11.6(12.5)	No		→ PL + MEKAL	
123557.8+275807	2001-01-14	1.4(1.5)	No	Transient?	[N/A]	Inner disc
	2001-06-04	2.6(2.9)	No			
123558.6+275742	2001-01-14	4.2(4.3)	**Yes**	Gradual fade or random?	MCDBB	Inner disc/bulge
	2001-06-04	8.9(9.1)	No			
132938.6+582506	2001-01-09	5.7(6.9)	No	Random	Soft PL	Inner disc
	2001-05-02	1.8(2.4)	No			

Notes: [a] Observed 0.5 – 8 keV luminosity in units of 10^{39} erg s^{-1}. Figures in parentheses are the intrinsic values. The luminosity of CXOU J120922.6+295551 is converted from the count rate assuming a powerlaw continuum with $\Gamma = 1.8$ and foreground absorption, whereas the luminosities for CXOU J123557.8+275807 are derived from a rough spectral fit to its second epoch data (an absorbed MCDBB with $N_H \sim 9 \times 10^{20}$ atoms cm^{-2} and $kT_{in} \sim 1.2$ keV). [b] We use PL as shorthand for a powerlaw continuum. [N/A] indicates that we did not have sufficient quality data for the analysis.

optically-thin thermal emission in the ULX spectrum, which is not present five months earlier. Since individual line features are not evident in the raw data, this interpretion is very model dependent and needs to be checked via future observations. Bearing in mind these caveats we can, nevertheless, speculate as to how such thermal emission might be produced.

The putative MEKAL component is emitting an incredible $\sim 2.7 \times 10^{39}$ erg s^{-1} of 0.5 –8 keV X-ray luminosity if the emission is isotropic. To place this is context, this an order of magnitude greater than the integrated diffuse luminosity of several small nearby galaxies (c.f. Read, Ponman & Strickland 1997). We note that CXOU J123551.7+275604 might not be an unique system; two other ULXs have been reported with possible thermal plasma components, with a similar very soft component reported on the basis of a joint *ROSAT* PSPC/*ASCA* spectral fit of the Holmberg II ULX by Miyaji, Lehmann & Hasinger (2001), and a much hotter and time-variable thermal component detected for an ULX in M51 (Terashima & Wilson 2003).

What processes might produce thin-thermal plasma emission in the X-ray spectrum of a ULX? Miyaji, Lehmann & Hasinger (2001) suggest the presence of one or more supernovae in the immediate environment of the Holmberg II ULX, but we can reject this for CXOU J123551.7+275604 given the rapid appearance of the plasma and the lack of a reported recent supernova at this position. In contrast, Terashima & Wilson (2003) draw an analogy to the X-ray spectrum of some HMXBs in eclipse, which are dominated by emission-lines that originate in photoionization of the stellar wind by the hard X-ray emission of the accreting primary (e.g. Cyg X-3; c.f. Liedahl & Paerels 1996). However, we cannot be observing thermal emission due to a reduction in contrast with the direct emission from the ULX, since we measure a higher overall flux in the second epoch observation when the plasma component is present. In any event, the plasma component we measure appears far too soft, at 0.18 keV, to be directly analogous to the photoionized stellar wind in sources such as Cyg X-3, which are typically identified by strong emission lines at energies well above 1 keV.

The emission measure of the plasma is $n_e^2 V = 2.9 \times 10^{63}$ cm^{-3}, where n_e is the electron density in atom cm^{-3} and V is the volume of the material. Since the plasma is optically thin, it must satisfy the limit $n_e r < \frac{1}{\sigma_T}$, where r is the pathlength through the plasma and σ_T is the Thompson scattering cross-section. Combining these two estimates gives $r_{min} \approx 3 \times 10^9$ km, implying that the plasma occupies a region far larger than the black hole accretion disc. However, as we argue above, it is probably too soft to be a photoionized stellar wind, which leaves the alternative possibility that it is a collisionally-ionized system. This could arise if an outflow from the ULX (perhaps in the form of a relativistic jet[5]) impacts upon a cloud of material relatively close to the ULX.

We further speculate that this scenario might occur if the secondary star in the system is an evolved high mass star, since these are known to eject discrete shells of material, for example with luminous blue variable (LBV) stars thought to lose up to 5×10^{-3} M$_\odot$ yr^{-1} in such discrete outburst events (van der Sluys & Lamers 2003 and references therein). For the derived value of r_{min} we calculate an electron density $n_{e,max} \approx 4.9 \times 10^9$ cm^{-3} and hence a mass of 4.8×10^{-4} M$_\odot$ for the plasma, well within the ejection masses quoted above. To energize this mass of material to a temperature of $kT = 0.18$ keV requires an energy input of $E = 3N_e kT$, where N_e is the total number of electrons in the plasma, hence a total of at least $\sim 4.8 \times 10^{44}$ erg is required. In the 141 days between the observations, this would require an average mechanical energy input from the outflow of at least $\sim 4 \times 10^{37}$ erg s^{-1}. We note that this energy input could be easily achievable by relativistic jets; for example the W50 radio bubble surrounding SS 433 probably originates in inflation by the mildly-relativistic jets of SS 433, with an average mechanical energy input from the jets of 3×10^{39} erg s^{-1}

[5] It is quite reasonable for an ULX to possess a relativistic jet regardless of whether or not it dominates the X-ray emission. By way of analogy, Galactic black hole systems such as GRS 1915+105 (i.e. microquasars) certainly do possess relativistic jets that do not dominate their X-ray emission.

(Dubner et al. 1998). Hence this scenario appears physically plausible.

Finally, we note that if the collisionally-excited material does originate in the ejection of matter from an evolved high-mass star, then this scenario is consistent with the suggestion of King et al. (2001) that ULXs are fed by thermal-timescale mass transfer from an evolved secondary star in a HMXB. However, it is not clear whether this system could be an "ordinary" HMXB containing a stellar-mass BH in accordance with the King et al. (2001) model, as Cropper et al. (2003) conclude that its observational characteristics point towards it containing an IMBH.

Clearly future monitoring of the behaviour of CXOU J123551.7+275604 is required to resolve many the uncertainties as to its nature and in particular to investigate whether outflow/stellar material collision events occur in reality.

6 CONCLUSIONS

In this paper we have studied dual-epoch observations of five nearby ULXs obtained with the *Chandra* ACIS-S detector. These have revealed heterogeneity in the observed properties of ULXs, from the characteristics of individual sources varying between the observation epochs, to a wide range of observed X-ray properties across the sample. The main outcomes of our analysis are:

- We detect all five target ULXs, though two have faded to luminosities below 10^{39} erg s^{-1}, plus we find three additional ULXs within the regions of the galaxies that we observe.
- The ULXs are all likely to be associated with the young stellar populations residing in and around the star forming regions of their host galaxies. This is consistent with the discovery of large ULX populations in starburst galaxies, extending the ULX – young stellar population link to "normal" spiral galaxies. We estimate that no more than two out of the eight ULXs originate in older stellar populations on the basis of the ULXs per unit optical luminosity measured in elliptical galaxies by Colbert & Ptak (2002).
- All the ULXs are point-like at the 0.5-arcsecond on-axis *Chandra* resolution.
- We derive the spectral parameters for six ULXs in both observational epochs, finding that the majority (five) are best fit by a powerlaw continuum rather than a MCDBB model, contrary to some previous reports for ULXs (e.g. Makishima et al. 2000). Two of the five best fit by powerlaws require an additional, very soft spectral component in at least one observation.
- Extreme short-term variability (on a timescale of hundreds of seconds) is observed in only two ULXs, and in these sources it is only seen in one of two observations. However, all the ULXs with archival data are variable by factors of a 2 – 4, over timescales of years.
- The lack of short-term variability, unless it occurs on timescales much less than our temporal sampling, may indicate that the X-ray emission of ULXs as a class is not dominated by relativistically-beamed jets.
- By utilising the new black hole state diagnostics of McClintock & Remillard (2003), we see that four out of the five powerlaw-dominated spectra have photon indices consistent with the low/hard state. This challenges the recent assertions that powerlaw-dominated spectra in ULXs originate in the very high state. However, if this truly is the low/hard state it could pose problems for interpretations of ULXs involving anisotropic stellar-mass black holes, and the simplest explanation would be that we are seeing a low/hard state from accretion onto an IMBH. The alternative is that we might be observing a state unique to the very high accretion rates required for stellar-mass black hole models.
- We find that equal numbers of ULXs (three apiece) show spectral "hardening" and "softening" with increasing luminosity. This indicates either an underlying physical heterogeneity in the ULX population, or perhaps that the bulk of the ULX population is composed of sources that can behave in both ways.
- The X-ray spectrum of CXOU J123551.7+275604 is particularly interesting, in that it is possible that a very soft and luminous MEKAL component appears in the five months between the two observations. We speculate that this plasma (if real) originates in the impact of an outflow (possibly relativistic jets) from the ULX on material in its close vicinity. One possible source of this material could be in discrete mass ejection events from an evolved high-mass secondary star. The presence of an evolved high-mass companion star is consistent with the scenario suggested by King et al. (2001), where many ULXs are ordinary HMXBs with an evolved high-mass secondary, though conversely this ULX is a very good candidate for an IMBH.

The properties outlined above portray ULXs as a class with very heterogeneous properties. Whilst some trends are emerging, such as the likely relation between many ULXs and young stellar populations, the lack of observable short-term variability, and a preference for powerlaw continuum spectra, none of these provide conclusive observational evidence to distinguish between the competing physical models. It could be that much of the confusion is because ULXs are a physically heterogeneous class, including both stellar-mass black holes, many of which could be in HMXBs, and IMBHs. Perhaps, then, the question we should be addressing is: to what degree are the ULX populations heterogeneous? An answer to this question is reliant upon future large samples of high-quality X-ray data, plus detailed multi-wavelength follow-up, to study these objects in much greater detail. It appears that we are still at the beginning of long road towards understanding these extraordinary X-ray sources.

ACKNOWLEDGMENTS

The authors would like to thank the anonymous referee for their comments, which have greatly improved the interpretation of our results. We would also like to thank Paulina Lira for an initial discussion on targets for this programme. TPR gratefully acknowledges support from PPARC. This research has made use of the NASA/IPAC Extragalactic Database (NED) which is operated by the Jet Propulsion Laboratory, California Institute of Technology, under contract with the National Aeronautics and Space Administration. This research has also made use of data obtained from the Leicester Database and Archive Service at the Department of Physics and Astronomy, Leicester University, UK. The second digitized sky survey was produced by the Space Telescope Science Institute, under Contract No. NAS 5-26555 with the National Aeronautics and Space Administration.

REFERENCES

Angelini L., Loewenstein M., Mushotzky R.F., 2001, ApJ, 557, L35
Bauer F.E., Brandt W.N., Sambruna R.M., Chartas G., Garmire G., Kaspi S., Netzer H., 2001, AJ, 122, 182
Baumgardt H., Hut P., Makino J., McMillan S., Portegies Zwart S., 2003, ApJ, 582, L21
Begelman M.C., 2002, ApJ, 568, L97
Bregman J.N., Cox C.V., Tomisaka K., 1993, ApJ, 415, L79
Bregman J.N., Glassgold A.E., 1982, ApJ, 263, 564

Bregman J.N., Pildis R., 1992, ApJ, 398, L107
Colbert E.J.M., Mushotzky R.F., 1999, ApJ, 519, 89
Colbert E.J.M., Ptak A.F., 2002, ApJS, 143, 25
Cropper M., Soria R., Mushotzky R.F., Wu K., Markwardt C.B., Pakull M., 2003, MNRAS, in press
Crosthwaite L.P., Turner J.L., Ho P.T.P., 2000, AJ, 119, 1720
Dahlem M., Heckman T.M., Fabbiano G., 1995, ApJ, 442, L49
Dahlem M., Heckman T.M., Fabbiano G., Lehnert M.D., Gilmore D., 1996, ApJ, 461, 724
Davis J.E., 2001, ApJ, 562, 575
de Vaucouleurs G., de Vaucouleurs A., Corwin H.G. Jr., Buta R.J., Paturel G., Fouqué P., 1991, Third reference catalogue of bright galaxies (New York: Springer)
Done C., Wardzinski G., Gierlinski M., 2003, MNRAS, submitted
Dubner G.M., Holdaway M., Goss W.M., Mirabel I.F., 1998, AJ, 116, 1842
Ebisuzaki T., et al., 2001, ApJ, 562, L19
Esin A.A., McClintock J.E., Narayan R., 1997, ApJ, 489, 865
Fabbiano G., Kim D.-W., Trinchieri G., 1992, ApJS, 80, 531
Fabbiano G., King A.R., Zezas A., Ponman T.J., Rots A., Schweizer F., 2003, ApJ, 591, 843
Fabbiano G., Trinchieri G., 1987, ApJ, 315, 46
Fabbiano G., Zezas A., King A.R., Ponman T.J., Rots A., Schweizer F., 2003, ApJ, 584, L5
Fabbiano G., Zezas A., Murray S.S., 2001, ApJ, 554, 1035
Falco E., et al., 1999, PASP, 111, 438
Gao Y., Wang Q.D., Appleton P.N., Lucas R.A., 2003, ApJ, 596, L171
Gebhardt K., Rich R.M., Ho L.C., 2002, ApJ, 578, L41
Georganopoulos M., Aharonian F.A., Kirk J.G., 2002, A&A, 388, L25
Gerssen J., van der Marel R.P., Gebhardt K., Guhathakurta P., Peterson R.C., Pryor C., 2002, AJ, 124, 3270
Goad M.R., Roberts T.P., Knigge C., Lira P., 2002, MNRAS, 335, L67
Ho L.C., Filippenko A.V., Sargent W.L.W., 1997, ApJS, 112, 315
Homan J., Wijnands R., van der Klis M., Belloni T., van Paradijs J., Klein-Wolt M., Fender R., Mendez M., 2001, ApJS, 132, 377
Immler S., Pietsch W., Aschenbach B., 1998, A&A, 331, 601
Irwin J.A., Athey A.E., Bregman J.N., 2003, ApJ, 587, 356
Kaaret P., Corbel S., Prestwich A.H., Zezas A., 2003, Science, 299, 365
Kaaret P., Prestwich A., Zezas A., Murray S., Kim D.-W., Kilgard R., Schlegel E., Ward M., 2001, MNRAS, 321, L29
King A., 2002, MNRAS, 335, L13
King A., 2003a, to appear in Compact Stellar X-ray Sources, eds. W.H.G. Lewin and M. van der Klis.
King A., 2003b, MNRAS, submitted
King A., Davies M.B., Ward M.J., Fabbiano G., Elvis M., 2001, ApJ, 552, L109
King A., Pounds K.A., 2003, MNRAS, 345, 657
Körding E., Falcke H., Markoff S., 2002, A&A, 382, L13
Krauss M., Kilgard R., Garcia M., Roberts T.P., Prestwich A., 2003, ApJ, submitted
Kubota A., Done C., Makishima K., 2002, MNRAS, 337, L11
Kubota A., Mizuno T., Makishima K., Fukazawa Y., Kotoku J., Ohnishi T., Tashiro M., 2001, ApJ, 547, L119
La Parola V., Damiani F., Fabbiano G., Peres G., 2003, ApJ, 583, 758
La Parola V., Peres G., Fabbiano G., Kim D.W., Bocchino F., 2001, ApJ, 556, 47
Liedahl D.A., Paerels F., 1996, ApJ, 468, L33
Lira P., Lawrence A., Johnson R.A., 2000, MNRAS, 319, 17
Lira P., Ward M.J., Zezas A., Alonso-Herrero A., Ueno S., 2002, MNRAS, 330, 259
Liu J.-F., Bregman J.N., Irwin J., Seitzer P., 2002, ApJ, 581, L93
Liu J.-F., Bregman J.N., Seitzer P., 2002, ApJ, 580, L31
Madau P., Rees M.J., 2001, ApJ, 551, L27
Makishima K. et al., 2000, ApJ, 535, 632
Mason K.O., et al., 2000, MNRAS, 311, 456
McClintock J.E., Remillard R.A., 2003, to appear in Compact Stellar X-ray Sources, eds. W.H.G. Lewin and M. van der Klis.
Miller J.M., Fabbiano G., Miller M.C., Fabian A.C., 2003, ApJ, 585, L40
Miller J.M., Fabian A.C., Miller M.C., 2003, ApJ, submitted
Miller M.C., Hamilton D.P., 2002, MNRAS, 330, 232
Mirabel I.F., Mignani R., Rodrigues I., Combi J.A., Rodriguez L.F., Guglielmetti F., 2002, A&A, 395, 595
Mirabel I.F., Rodriguez L.F., 1999, ARA&A, 37, 409
Misra R., Sriram K., 2003, ApJ, 584, 981
Mitsuda K., et al., 1984, PASJ, 36, 741
Miyaji T., Lehmann I., Hasinger G., 2001, AJ, 121, 3041
Mizuno T., Kubota A., Makishima K., 2001, ApJ, 554, 1282
Mukai K., Pence W.D., Snowden S.L., Kuntz K.D., 2003, ApJ, 582, 184
Okada K., Dotani T., Makishima K., Mitsida K., Mihara T., 1998, PASJ, 50, 25
Portegies Zwart S.F., McMillan S.L.W., 2002, ApJ, 576, 899
Pottschmidt K., Wilms J., Nowak M.A., Pooley G.G., Gleissner T., Heindl W.A., Smith D.M., Remillard R., Staubert R., 2003, A&A, 407, 1039
Read A.M., Ponman T.J., Strickland D.K., 1997, MNRAS, 286, 626
Reynolds C.S., Loan A.J., Fabian A.C., Makishima K., Brandt W.N., Mizuno T., 1997, MNRAS, 286, 349
Roberts T.P., Colbert E.J.M., 2003, MNRAS, 341, L49
Roberts T.P., Goad M.R., Ward M.J., Warwick R.S., O'Brien P.T., Lira P., Hands A.D.P., 2001, MNRAS, 325, L7
Roberts T.P., Goad M.R., Ward M.J., Warwick R.S., 2003, MNRAS, 342, 709
Roberts T.P., Warwick R.S., 2000, MNRAS, 315, 98 (RW2000)
Roberts T.P., Warwick R.S., Ward M.J., Murray S.S., 2002, MNRAS, 337, 677
Stark A., Gammie C.F., Wilson R.W., Bally J., Linke R.A., Heiles C., Hurwitz M., 1992, ApJS, 79, 77
Strickland D.K., Colbert E.J.M, Heckman T.M., Weaver K.A., Dahlem M., Stevens I.R., 2001, ApJ, 560, 707
Sugiho M., Kotoku J., Makishima K., Kubota A., Mizuno T., Fukazawa Y., Tashiro M., 2001, ApJ, 561, L73
Terashima Y., Wilson A., 2003, ApJ, submitted
Tully R.B., 1988, Nearby Galaxies Catalog, Cambridge: Cambridge University Press
van der Marel R.P., Gerssen J., Guhathakurta P., Peterson R.C., Gebhardt K., Pryor C., 2002, AJ, 124, 3255
van der Sluys M.V., Lamers H.J.G.L.M., 2003, A&A, 398, 181
Veron-Cetty M.-P., Veron P., 2000, Quasars and Active Galactic Nuclei (9th edition), ESO Sci. Rep., 19, 1
Voges W., et al., 1999, A&A, 349, 389
Vogler A., Pietsch W., Bertoldi F., 1997, A&A, 318, 768
Yaqoob T., Serlemitsos P.J., Ptak A., Mushotzky R., Kunieda H., Terashima Y., 1995, ApJ, 455, 508
Zezas A., Fabbiano G., 2002, ApJ, 577, 726
Zezas A., Fabbiano G., Rots A.H., Murray S.S., 2002, ApJ, 577, 710
Zezas A., Ward M.J., Murray S.S., 2003, ApJ, 594, L31

APPENDIX A: PREVIOUS OBSERVATIONS OF THE ULXS

A1 IC 342 X-1 (CXOU J034555.7+680455)

This ULX was first detected in an *Einstein* IPC observation of IC 342, with a 0.2 – 4 keV X-ray luminosity of 3×10^{39} erg s^{-1} (Fabbiano & Trinchieri 1987). A subsequent *ROSAT* HRI observation detected IC 342 X-1 in a similarly luminous state (Bregman, Cox & Tomisaka 1993; RW2000). An early *ASCA* observation showed IC 342 X-1 to be in a very luminous, highly variable state, in which its average 0.5 – 10 keV luminosity surpassed 10^{40} erg s^{-1} and it displayed large amplitude variability on $\sim$ 1000 s timescales (Okada et al. 1997). In this state its X-ray spectrum was well-fit by the multi-colour disc blackbody model describing an accretion disc around a black hole in a high/soft state (Makishima et al. 2000). However, a follow-up observation obtained late in the *ASCA* mission showed the ULX to have dimmed to a luminosity of 6×10^{39} erg s^{-1} and undergone a spectral transition to a

low/hard state, similar to the behaviour observed in many Galactic and Magellanic black hole X-ray binary systems (Kubota et al. 2001; Mizuno, Kubota & Makishima 2001). However, the low/hard spectral state has recently been re-interpreted as a high/anomalous state where the X-ray spectrum is described by a strongly Comptonised optically thick accretion disc, as observed in many Galactic black-hole X-ray binaries experiencing a high mass accretion rate (Kubota, Done & Makishima 2002). Finally, recent William Herschel Telescope integral field unit observations have revealed that this ULX lies at the centre of a large nebula, probably a supernova remnant shell (Roberts et al. 2003 and references therein). The inferred initial energy input to the SNR is consistent with a hypernova event, and highly excited [OIII] emission-line regions on the inner edge of the shell suggest that the ULX is photoionizing its inner regions to produce an X-ray ionized nebula.

A2 NGC 3628 X-2 (CXOU J112037.3+133429)

This source was first detected as "point source 2" in a December 1979 *Einstein* IPC image of NGC 3628, as reported by Bregman & Glassgold (1982), where it was observed to lie at the eastern end of the edge-on galaxy disc. They derived a 0.3 - 2.9 keV luminosity of 2.1×10^{39} erg s^{-1} for NGC 3628 X-2, corrected to our assumed a distance of 7.7 Mpc (this correction is assumed for all the following luminosities). However, the reprocessed IPC data contour map presented by Fabbiano, Kim & Trinchieri (1992) suggests, in retrospect, that this flux may be an upper limit due to confusion with two X-ray sources since resolved to the north of X-2[6]. It was also detected in three separate *ROSAT* observations, once with the PSPC and twice with the HRI, as reported in Dahlem, Heckman & Fabbiano (1995) and Dahlem et al. (1996). In particular, the November 1991 PSPC observation provides a measurement of its X-ray luminosity in the 0.1 - 2 keV band of 0.6×10^{39} erg s^{-1}, several times lower than the *Einstein* value. This apparent variability is supported by the *ROSAT* HRI images, which demonstrate that the count rate of NGC 3628 X-2 drops substantially between December 1991 and May 1994. NGC 3628 X-2 was also detected in a December 1993 *ASCA* observation (Yaqoob et al. 1995). Its *ASCA* SIS spectrum was well-fit with a simple powerlaw continuum model, with $\Gamma \sim 2.4$ and an absorption column of $N_H \sim 7 \times 10^{21}$ atoms cm^{-2}, well in excess of the foreground Galactic column. This model implies luminosities of 0.7 and 1.7×10^{39} erg s^{-1} in the 0.5 – 2 and 2 – 10 keV bands respectively, consistent with the *ROSAT* PSPC measurement in the soft X-ray regime, though this must again be regarded as an upper limit due to the likelihood of confusion with other sources in the wide *ASCA* beam. Yaqoob et al. (1995) comment that the X-ray spectrum of NGC 3628 X-2 is consistent with either a low-mass X-ray binary or a very young supernova remnant, noting that if it is an accreting source then it is substantially super-Eddington for a 1 $M_\odot$ object. Finally, NGC 3628 X-2 was not covered in the previous *Chandra* ACIS-S observation of NGC 3628 discussed by Strickland et al. (2001), as their observation was aligned along the minor axis of the galaxy.

[6] These sources are now identified as the QSO J112041.7+133552 (Veron-Cetty & Veron 2000), and a narrow emission-line galaxy RIXOS 259- 7 (Mason et al. 2000).

A3 NGC 4136 X-1 (CXOU J120922.6+295551)

The first and, previous to this work, only detection of this ULX was made by Lira, Lawrence & Johnson (2000), who obtained a luminosity of 2.5×10^{39} erg s^{-1} (corrected to a distance of 9.7 Mpc) from a *ROSAT* HRI observation of NGC 4136. They note that its position is coincident with a diffuse blue optical counterpart, which may be emission knots in the spiral arms of the galaxy.

A4 NGC 4559 X-1 (CXOU J123551.7+275604) & X-4 (CXOU J123558.6+275742)

NGC 4559 X-1 was first detected in the *ROSAT* all-sky survey bright source catalogue as 1RXS J123551.6+275555 (Voges et al. 1999). It was identified with the outer edge of the galactic disc of NGC 4559 by Vogler, Pietsch & Bertoldi (1997), who present a detailed analysis of the X-ray properties of this source based on a *ROSAT* PSPC pointed observation. In their work they refer to this source as NGC 4559 X-7. The PSPC profile of the source is point-like, and no significant X-ray variability is detected from it during the observation. Its spectrum is well-fit by either a powerlaw continuum ($\Gamma \sim 3$) or thermal bremsstrahlung model ($kT \sim 0.8$ keV), both showing absorption $N_H \sim 1 - 2 \times 10^{21}$ atoms cm^{-2}, well in excess of the foreground galactic column. The observed (0.1 - 2.4 keV) luminosity of 6×10^{39} erg s^{-1} converts to an impressive intrinsic luminosity of 1.5×10^{40} erg s^{-1} using the thermal bremsstrahlung model. The PSPC position is coincident with a group of emission knots in a faint outer spiral arm of the galaxy, which Vogler et al. identify as likely HII regions. It is, however, too bright to be the integrated X-ray emission of "ordinary" X-ray binaries and supernova remnants associated with the HII region. They conject that this source is most likely a supernova remnant buried in a dense cloud of interstellar material, though they do not rule out either a black-hole accreting binary system, or mini-AGN from a merging dwarf galaxy, as alternative identifications. This source was also detected, with a similar high X-ray luminosity, in a *ROSAT* HRI observation (RW2000).

Unlike NGC 4559 X-1, NGC 4559 X-4 was not detected in the *ROSAT* all-sky survey bright source catalogue. However, in the *ROSAT* PSPC observation reported by Vogler et al. (who list this ULX as NGC 4559 X-10) it was brighter than X-1. It is located near, but not at, the centre of the galaxy. It appears as an extended source in the PSPC observation, with about 20% of its flux emanating from between 20 and 50 arcseconds from the source centroid, which may be a diffuse component, or confusion with other point sources (with our *Chandra* data suggesting the latter). The X-ray spectrum is well-fit by either a powerlaw continuum, or thermal bremsstrahlung emission, albeit spectrally harder in each case than for X-1 ($\Gamma \sim 2.0$, or $kT \sim 2.1$ keV, respectively), with a measured absorption column of $N_H \sim 10^{21}$ atoms cm^{-2}. This gave an observed (intrinsic) luminosity of $7(12) \times 10^{39}$ erg s^{-1}. Vogler et al. suggest that X-10 is the superposition of several point sources, though they cannot rule out the contribution of an AGN towards the observed flux. This source is again also detected in the *ROSAT* HRI survey of RW2000, offset from the nucleus of NGC 4559 by 13 arcseconds.

A5 NGC 5204 X-1 (CXOU J132938.6+582506)

This ULX was first detected in an *Einstein* IPC observation, with a 0.2 – 4 keV X-ray luminosity of $\sim 2.6 \times 10^{39}$ erg s^{-1} (Fabbiano, Kim & Trinchieri 1992). It also appeared in the *ROSAT* all-

sky survey bright source catalogue with a count rate of $7.5 \times 10^{-2}\,\mathrm{count\,s^{-1}}$. Later *ROSAT* HRI pointed observations revealed NGC 5204 X-1 to lie ~ 20 arcseconds to the east of the nucleus of NGC 5204 (Colbert & Mushotzky 1999; RW2000; Lira, Lawrence & Johnson 2000). This ULX was revealed to have a point-like optical counterpart with a blue continuum spectrum in a William Herschel Telescope integral field observation (Roberts et al. 2001), suggestive of the presence of several O-stars. A more detailed study using archival *HST* data resolved the ULX into three possible counterparts, all of which are consistent with young (< 10 Myr old) compact stellar clusters in NGC 5204, suggesting that this ULX may be a high-mass X-ray binary system (Goad et al. 2002).